The Astronomical Journal, 151:78 (20pp), 2016 March doi:10.3847/0004-6256/151/3/78

JELLYFISH GALAXY CANDIDATES AT LOW REDSHIFT

B. M. Poggianti[1], G. Fasano[1], A. Omizzolo[1,2], M. Gullieuszik[1], D. Bettoni[1], A. Moretti[3], A. Paccagnella[1,3], Y. L. Jaffé[4], B. Vulcani[5], J. Fritz[6], W. Couch[7], and M. D'Onofrio[3]
[1] INAF-Astronomical Observatory of Padova, Italy
[2] Vatican Observatory, Vatican City State
[3] Physics and Astronomy Department, University of Padova, Italy
[4] Department of Astronomy, Universidad de Concepción, Concepción, Chile
[5] Kavli Institute for the Physics and Mathematics of the universe (WPI), The University of Tokyo Institutes for Advanced Study (UTIAS), the University of Tokyo, Kashiwa, 277-8582, Japan
[6] Centro de Radioastronomía y Astrofísica, CRyA, UNAM, Michoacán, Mexico
[7] Australian Astronomical Observatory, North Ryde, NSW 1670, Australia
Received 2015 July 10; accepted 2015 November 15; published 2016 February 25

ABSTRACT

Galaxies that are being stripped of their gas can sometimes be recognized from their optical appearance. Extreme examples of stripped galaxies are the so-called "jellyfish galaxies" that exhibit tentacles of debris material with a characteristic jellyfish morphology. We have conducted the first systematic search for galaxies that are being stripped of their gas at low-z ($z = 0.04-0.07$) in different environments, selecting galaxies with varying degrees of morphological evidence for stripping. We have visually inspected B- and V-band images and identified 344 candidates in 71 galaxy clusters of the OMEGAWINGS+WINGS sample and 75 candidates in groups and lower mass structures in the PM2GC sample. We present the atlas of stripping candidates and a first analysis of their environment and their basic properties, such as morphologies, star formation rates and galaxy stellar masses. Candidates are found in all clusters and at all clustercentric radii, and their number does not correlate with the cluster velocity dispersion σ or X-ray luminosity L_X. Interestingly, convincing cases of candidates are also found in groups and lower mass halos ($10^{11}-10^{14} M_\odot$), although the physical mechanism at work needs to be securely identified. All the candidates are disky, have stellar masses ranging from $\log M/M_\odot < 9$ to > 11.5 and the majority of them form stars at a rate that is on average a factor of 2 higher (2.5σ) compared to non-stripped galaxies of similar mass. The few post-starburst and passive candidates have weak stripping evidence. We conclude that disturbed morphologies suggestive of stripping phenomena are ubiquitous in clusters and could be present even in groups and low mass halos. Further studies will reveal the physics of the gas stripping and clarify the mechanisms at work.

Key words: atlases – galaxies: clusters: intracluster medium – galaxies: evolution – galaxies: groups: general – galaxies: ISM – galaxies: star formation

Supporting material: data behind figure, figure set, machine-readable tables

1. INTRODUCTION

In order to unveil the physical drivers of galaxy evolution, it is crucial to study the processes of gas acquisition and loss. Gas is the fuel for star formation (SF) and a sensitive tracer of environmental effects.

Gas loss from galaxies can be caused by mechanisms internal to galaxies themselves, such as galactic winds due to SF or an active galactic nucleus (e.g., Veilleux et al. 2005; Fogarty et al. 2012; Ho et al. 2014). In addition, several external mechanisms that can potentially impact on a galaxy gas content have been proposed (Boselli & Gavazzi 2006; De Lucia 2010). Among those not directly affecting the galaxy stellar component, there are ram pressure stripping from the disk due to the interaction between the galaxy interstellar medium (ISM) and the intergalactic medium (IGM, Gunn & Gott 1972), and the removal of the hot gas halo surrounding the galaxy (the so-called "strangulation") either via ram pressure or via tidal stripping by the halo potential (Larson et al. 1980; Balogh et al. 2000). While the first one partially or completely removes the ISM, the second one deprives the galaxy of its gas reservoir, and leaves the existing ISM in the disk to be consumed by SF. Circumgalactic gas can also be shock-heated and, as a consequence, can stop cooling in dark matter halos above a critical mass (Dekel & Birnboim 2006). Other, less often cited, processes that can be as or even more efficient in certain conditions are thermal evaporation (Cowie & Songaila 1977) and turbulent/viscous stripping (Nulsen 1982). Among those processes that affect both gas and stars, instead, there are strong tidal interactions and minor and major mergers (expected to be more common in groups, Barnes & Hernquist 1992; Mihos & Hernquist 1994), tidal effects of the cluster as a whole (Byrd & Valtonen 1990) and "harassment," i.e., the cumulative effect of several weak and fast tidal encounters, expected to be more efficient in galaxy clusters (Moore et al. 1996).

Some of the most striking examples of gas stripping come from neutral hydrogen studies. Neutral hydrogen gas has been observed to be disturbed and eventually truncated and exhausted in galaxies in dense environments, such as clusters (Davies & Lewis 1973; Haynes et al. 1984; Giovanelli & Haynes 1985; Cayatte et al. 1990; Bravo-Alfaro et al. 2001; Kenney et al. 2004; Chung et al. 2009; Jaffé et al. 2015) and groups (Williams & Rood 1987; Verdes-Montenegro et al. 2001; Rasmussen et al. 2006, 2008; Sengupta & Balasubramanyam 2006). These studies point to ram pressure stripping, or a combination of ram pressure and tidal effects, as cause of the gas depletion.

Extreme examples of gas stripping are the so-called "jellyfish galaxies" (e.g., Ebeling et al. 2014; Fumagalli et al. 2014). They exhibit "tentacles" of material that appear to be stripped from the main body of the galaxy, and whose morphology is suggestive of gas-only removal mechanisms, such as ram pressure stripping. Jellyfish galaxies (with different naming) have been known in nearby clusters for many years. Usually, only a few galaxies per cluster have been studied, in a handful of clusters (e.g., Virgo, Coma, A1367, A3627, Shapley; Kenney & Koopmann 1999; Sun et al. 2006; Yoshida et al. 2008; Hester et al. 2010; Smith et al. 2010; Yagi et al. 2010; Merluzzi et al. 2013; Kenney et al. 2014). A few examples have been identified in clusters at $z \sim 0.2-0.4$ (Cortese et al. 2007; Owers et al. 2012; Ebeling et al. 2014; Rawle et al. 2014), and there is accumulating evidence for a correlation between the efficiency of the stripping phenomenon and the presence of shocks and strong gradients in the X-ray IGM (Owers et al. 2012; Vijayaraghavan & Ricker 2013). Known jellyfishes are star-forming or post-starburst galaxies; the existence of ellipticals with X-ray tails might be a different side of the same coin (e.g., Sun et al. 2005; Machacek et al. 2006).

Hα maps of jellyfish galaxies show tails of ionized gas up to 150 kpc long, where new stars are born in knots and end up contributing to the intracluster light. A recent MUSE study of a jellyfish in a cluster at $z = 0.016$ has ruled out gravitational interactions as mechanism for the gas removal and showed that ram pressure has removed the galaxy ISM from the outer disk, while the primary Hα tail is still being fed by gas from the galaxy inner regions (Fumagalli et al. 2014).

The goal of this paper is to present the results of a systematic search for galaxies whose optical morphology suggests they might be experiencing stripping of their gaseous material. By doing this, we aim to select all possible gas stripping candidates, from the most extreme cases (with classical "jellyfish" morphology) to examples without obvious "tentacles" but with morphologies and/or surrounding debris suggestive of stripping and/or ram pressure events. This search has been conducted in galaxy clusters and in the general field at $z = 0.04-0.07$, based on optical images of the OMEGAWINGS+WINGS (Fasano et al. 2006; Gullieuszik et al. 2015) and PM2GC (Calvi et al. 2011) samples described in Section 2. The process and criteria for candidate selection is presented in Section 3, and the methods to derive star formation rates (SFRs) and morphologies in Section 3.1. This paper presents the atlas of images and the catalogs (Section 4), the environments (Section 5), the morphologies and stellar population properties (SFRs, stellar masses, colors and spectral types) of 419 stripping candidates (Section 6).

In this paper we use $\Omega_m = 0.3$, $\Omega_\Lambda = 0.7$, $H_0 = 70\,\mathrm{km\,s^{-1}}$ $\mathrm{Mpc^{-1}}$ and a Kroupa (2001) IMF.

2. DATASETS

2.1. WINGS and OMEGAWINGS

WINGS is a large survey targeting 76 clusters of galaxies selected on the basis of their X-ray luminosity (Ebeling et al. 1996, 1998, 2000), covering a wide range in cluster masses ($\sigma = 500$–$1200+$ $\mathrm{km\,s^{-1}}$, $\log L_X = 43.3-45\,\mathrm{erg\,s^{-1}}$, Fasano et al. 2006). The original WINGS data set consisted of B and V deep photometry of a $34' \times 34'$ field of view with the WFC@INT and the WFC@2.2mMPG/ESO (Varela et al. 2009), spectroscopic follow-ups with 2dF@AAT and WYFFOS@WHT (Cava et al. 2009), plus J and K imaging with WFC@UKIRT (Valentinuzzi et al. 2009) and some U-band imaging (Omizzolo et al. 2014). This database is presented in Moretti et al. (2014) and has been employed for a number of studies (see https://sites.google.com/site/wingsomegawings/).

OMEGAWINGS is a recent extention of this project, that quadruples the area covered (1 square degree) and allows to reach up to ~2.5 cluster virial radii. OMEGAWINGS is based on two OmegaCAM@VST GTO programs for 46 WINGS clusters: a B and V campaign completed in P93, and an ongoing u-band programme. The B and V data, the data reduction and the photometric catalogs are presented in Gullieuszik et al. (2015). Spectra are obtained with AAOmega@AAT on the OmegaCAM field. So far, we have secured high quality spectra for ~30 OMEGAWINGS clusters, reaching very high spectroscopic completeness levels for galaxies brighter than $V = 20$ from the cluster cores to their periphery (A. Moretti et al. 2016, in preparation). Galaxies are considered cluster members if they are within 3σ from the cluster redshift. The mean redshift uncertainty, computed from the differences between WINGS and OMEGAWINGS redshift values of repeated objects, is $\Delta z = 0.0002$.

For this paper we consider the 41 OMEGAWINGS clusters with an OmegaCAM B and/or V-band seeing $\leqslant 1.2$ arcsec, listed in Table 1. Due to the segmentation of the B and V OmegaCAM filters, the OmegaCAM images have a central vignetting cross (Gullieuszik et al. 2015): only in the vignetted area we used the old WINGS images (Fasano et al. 2006). Finally, to complete the search within the WINGS sample, we used the old WINGS images for other 31 clusters not observed with OmegaCAM (Table 1). In the following, we keep these clusters separate from the rest because the WINGS imaging covers only the cluster cores (the central ~0.3 sq. deg.). The masses of OMEGAWINGS and WINGS clusters have been estimated from the σ applying the virial theorem according to Equation (4) in Poggianti et al. (2006).

2.2. PM2GC

The reference comparison field sample for WINGS and OMEGAWINGS is the Padova Millennium Galaxy and Group Catalog (PM2GC, Calvi et al. 2011), built from the Millennium Galaxy Catalogue (MGC, Liske et al. 2003), a deep 38 $\mathrm{deg^2}$ INT B-imaging survey with a highly complete spectroscopic follow-up (96% at $B = 20$, Driver et al. 2005). The image quality (for depth, pixel size, median seeing) and the spectroscopic completeness of the PM2GC are superior to Sloan, and these qualities result in more robust morphological classifications and better sampling of dense regions. This, and the fact that the observational data is very similar to WINGS and was analyzed in the same way with the same tools, make the PM2GC the ideal field counterpart for WINGS. The characterization of the environment of PM2GC galaxies was conducted by means of a Friends-of-friends algorithm by Calvi et al. (2011), who identified 176 groups of galaxies with at least three members[8] as well as binary systems and "single" galaxies, respectively defined as galaxies with just one or no neighbor

[8] A galaxy is considered member of a group if its spectroscopic redshift lies within 3σ from the median group redshift and if it is located within a projected distance of $1.5R_{200}$ from the group geometrical center. R_{200} is defined as the radius delimiting a sphere with interior mean density 200 times the critical density of the universe at that redshift. R_{200} is commonly used as an approximation of the group/cluster virial radius and is computed from the group or cluster velocity dispersion as in Poggianti et al. (2006).

Table 1
OMEGAWINGS (O) and WINGS (W) Clusters

Sample	Cluster	Redshift	σ (km s^{-1})	Log(L_X) (0.1–2.4 keV)	$N_{candidates}$
O	A1069	0.0651	677 ± 52	43.98	2
O	A119	0.0444	862 ± 52	44.51	7
O	A147	0.0447	666 ± 13	43.73	8
O	A151	0.0532	760 ± 55	44.00	5
O	A160	0.0438	561 ± 53	43.58	5
O	A1631a*	0.0465	750 ± 28	43.86	4
O	A168	0.0448	503 ± 43	44.04	6
O	A193	0.0484	777 ± 72	44.19	1
O	A1983	0.0447	527 ± 38	43.67	3
O	A1991	0.0584	599 ± 57	44.13	6
O	A2107	0.0410	592 ± 62	44.04	4
O	A2382	0.0639	699 ± 30	43.96	2
O	A2399	0.0577	722 ± 35	44.00	3
O	A2415	0.0575	696 ± 51	44.23	7
O	A2457	0.0587	685 ± 36	44.16	3
O	A2589	0.0419	816 ± 88	44.27	5
O	A2593	0.0417	701 ± 60	44.06	6
O	A2657	0.0400	381 ± 83	44.20	2
O	A2665	0.0562	⋯	44.28	1
O	A2734	0.0624	555 ± 42	44.41	2
O	A3128	0.0603	854 ± 28	44.33	4
O	A3158	0.0594	997 ± 38	44.73	4
O	A3266	0.0595	1309 ± 39	44.79	1
O	A3395	0.0507	1206 ± 55	44.45	4
O	A3528*	0.0535	899 ± 64	44.12	4
O	A3530*	0.0548	700 ± 40	43.94	5
O	A3532*	0.0555	621 ± 53	44.45	4
O	A3556*	0.0480	640 ± 35	43.97	1
O	A3558*	0.0485	1049 ± 52	44.80	14
O	A3560*	0.0489	710 ± 41	44.12	8
O	A3667	0.0558	1011 ± 42	44.94	2
O	A3716	0.0457	842 ± 27	44.00	2
O	A3809	0.0626	558 ± 38	44.35	2
O	A3880	0.0585	531 ± 35	44.27	7
O	A4059	0.0480	715 ± 59	44.49	4
O	A754	0.0545	1039 ± 63	44.90	3
O	A85	0.0521	1052 ± 68	44.92	3
O	A957x	0.0451	710 ± 53	43.89	3
O	IIZW108	0.0487	617 ± 42	44.34	2
O	MKW3s	0.0444	539 ± 37	44.43	1
O	Z8852	0.0408	765 ± 63	43.97	2
W	A133	0.0603	810 ± 78	44.55	5
W	A311	0.0657	⋯	43.91	2
W	A376	0.0476	852 ± 49	44.14	1
W	A500	0.0678	658 ± 48	44.15	4
W	A602	0.0621	720 ± 73	44.05	1
W	A671	0.0507	906 ± 58	43.95	1
W	A1291	0.0509	429 ± 49	43.64	1
W	A1644	0.0467	1080 ± 54	44.55	15
W	A1668	0.0634	649 ± 57	44.20	8
W	A1736	0.0461	853 ± 60	44.37	14
W	A1795	0.0633	725 ± 53	45.05	9
W	A1831	0.0634	543 ± 58	44.28	1
W	A2124	0.0666	801 ± 64	44.13	6
W	A2149	0.0675	353 ± 53	43.92	3
W	A2169	0.0578	509 ± 40	43.65	4
W	A2256	0.0581	1273 ± 64	44.85	4
W	A2572a	0.0390	631 ± 10	44.01	1
W	A2622	0.0610	696 ± 55	44.03	1
W	A2626	0.0548	625 ± 62	44.29	3
W	A2717	0.0498	553 ± 52	44.00	1
W	A3164	0.0611	⋯	44.17	2
W	A3376	0.0461	779 ± 49	44.39	2
W	A3490	0.0688	694 ± 52	44.24	4
W	A3497	0.0680	726 ± 47	44.16	4
W	RX0058	0.0484	637 ± 97	43.64	3
W	RX1022	0.0548	577 ± 49	43.54	1
W	RX1740	0.0441	582 ± 65	43.70	3
W	Z1261	0.0644	⋯	43.91	4
W	Z2844	0.0503	536 ± 53	43.76	1
W	Z8338	0.0494	712 ± 60	43.90	2

Note. Name, redshift, σ, L_X and number of stripping candidates (spectroscopic members or possible members, i.e., without redshift) of OMEGAWINGS and WINGS clusters. Those with an asterisk belong to the Shapley supercluster.

(This table is available in machine-readable form.)

with a projected mutual distance of $\leqslant 0.5\,h^{-1}$ Mpc and a redshift within 1500 km s^{-1}. The masses of the dark matter halos hosting PM2GC galaxies were estimated from the correlation between the dark matter halo mass and the total stellar mass of member galaxies (A. Paccagnella et al. 2015, in preparation).

3. DATA ANALYSIS

Two or three of us (first independently, then together) visually inspected the OMEGAWINGS and PM2GC (GF and BP) and WINGS-only (AO, GF and BP) B-band images searching for galaxies with optical evidence for gas stripping.[9] We searched for any type of evidence suggestive of gas stripping, selecting galaxies that have (a) debris trails, tails or surrounding debris located on one side of the galaxy and/or (b) asymmetric/disturbed morphologies suggestive of unilateral external forces, and/or (c) a distribution of star-forming regions and knots suggestive of triggered SF on one side of the galaxy. These criteria are similar to those used in previous studies of jellyfish galaxies (e.g., Ebeling et al. 2014).

For OMEGAWINGS+WINGS we inspected the whole image of each cluster, and inspected all galaxies in the image, without knowing their magnitude and whether they had a measured redshift. This selection yielded candidates with a B-band Sextractor AUTO magnitude (corrected for Galactic extinction) $\leqslant 20$ (Gullieuszik et al. 2015). For the PM2GC, instead, we looked at all galaxies with a spectroscopic redshift in the same range of WINGS clusters ($z = 0.04-0.07$), thus starting from the spectroscopic MGC catalog that has a limit $B = 20$. Thus, the classification process was done blindly with respect to environment: the classifier knew neither whether the galaxy was a cluster/group member, nor the distance to the cluster or group center. He/she only knew whether the image was from OMEGAWINGS, WINGS or PM2GC.

The images were first inspected independently by each classifier, who assigned a class according to the scheme described below. The different classifiers agreed to within one class in 83% of the cases. Then, each galaxy was inspected together by the common classifiers to ensure homogeneity, the final classification was agreed upon and a consensus was found

[9] For OMEGAWINGS, the V-band image was used if the median B-band seeing for that cluster was worse than 1.2 arcsec.

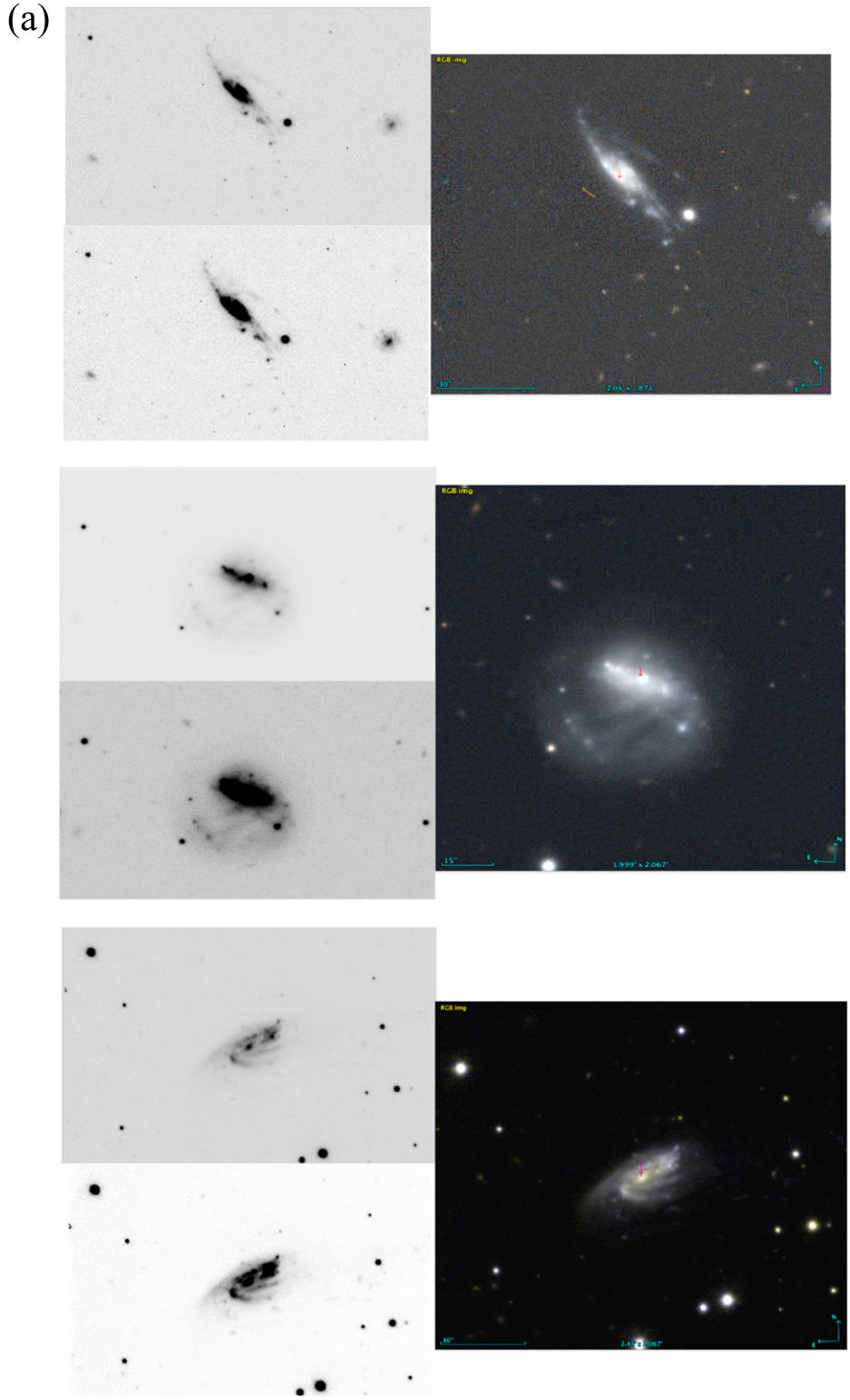

Figure 1. (a) JClass=5 OMEGAWINGS stripping candidates. Left Single filter images with two different level cuts. Right Color-composite image. (b) JClass=5 OMEGAWINGS candidates. (c) JClass=5 OMEGAWINGS candidates. (d) Examples of JClass=4 OMEGAWINGS candidates. (e) Examples of JClass=4 OMEGAWINGS candidates. (f) Examples of JClass=3 (top), JClass=2 (middle) and JClass=1 (bottom) OMEGAWINGS candidates. The JClass=1 galaxy is the one studied in Merluzzi et al. (2013).

A complete figure set (211 images) and the data used to create this figure are available.

on the classification of those galaxies whose individual class differed by more than one class.

We tentatively assigned our candidates to five classes according to the visual evidence for stripping signatures in the optical bands (JClass), from extreme cases (JClass 5) to progressively weaker cases, down to the weakest (JClass 1). As a result, our JClass=5 and 4 classes comprise the most secure candidates, and contain the most striking classical jellyfish

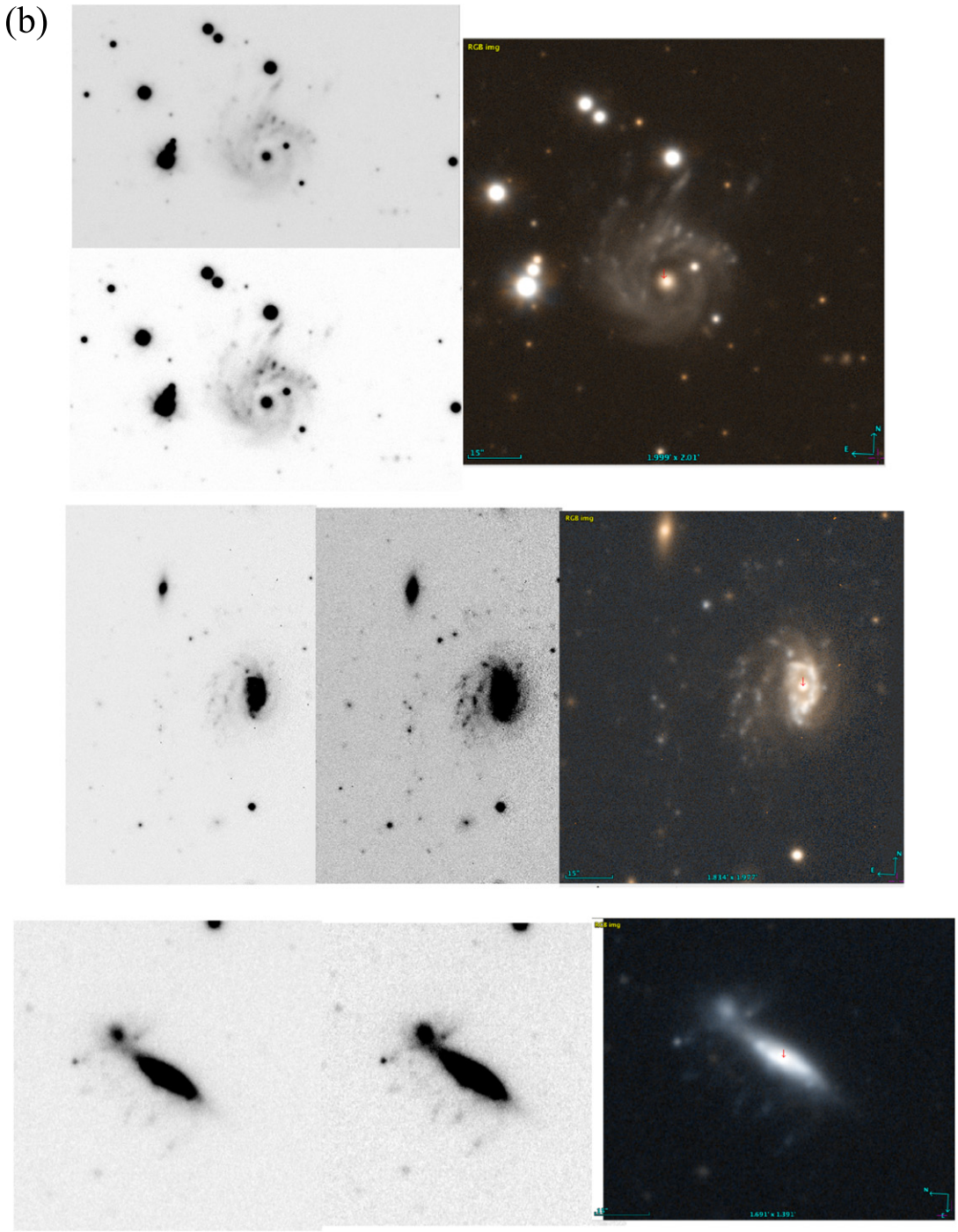

Figure 1. (Continued.)

galaxies. JClass 3 candidates are probable cases of stripping and/or ram pressure events, while JClasses 2 and 1 are tentative candidates, for which definitive conclusions cannot be reached on the basis of the existing imaging.

To this concern, however, it is interesting to note that integral-field spectroscopy of one of our weakest-class candidates (JClass 1) clearly shows one-sided extraplanar ionized gas stripped by ram pressure (Merluzzi et al. 2013). This galaxy, shown at the bottom of Figure 1, was selected by our visual inspection as a JClass = 1 and was later recognized as the galaxy studied by Merluzzi et al. (see Figures 5–7 in their paper for the outstanding stripped Hα-emitting gas on one side of it). In general, spatially resolved gas-sensitive studies of galaxies in the process of being stripped have shown that the optical signatures are just the tip of the iceberg (e.g., Merluzzi et al. 2013; Fumagalli et al. 2014; Kenney et al. 2015): the ongoing stripping is much more evident from the ionized gas than in the optical. This leads us to suspect that stripping takes place even in the optically weakest cases, and it is the reason why we deemed it useful to include in our catalog galaxies over the whole range of degree of evidence for stripping.

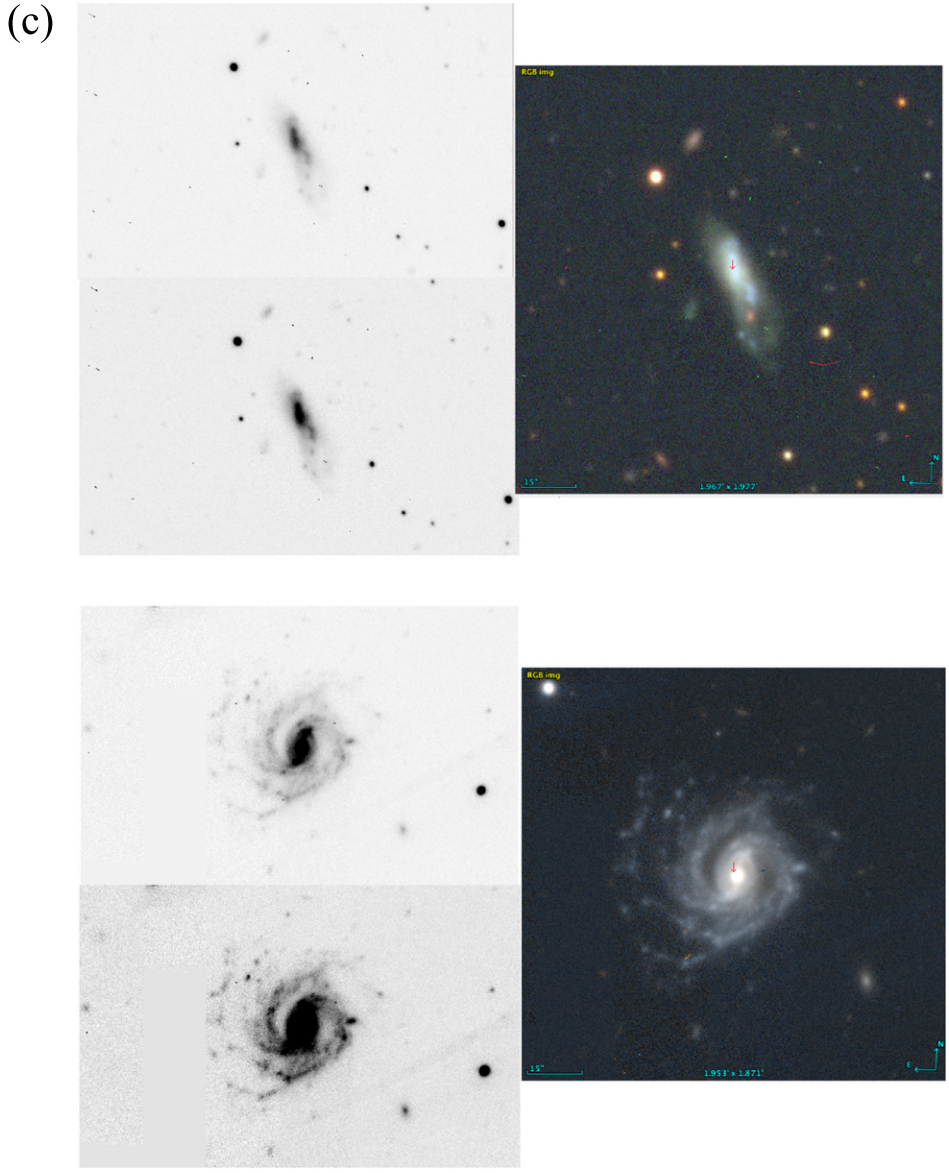

Figure 1. (Continued.)

Instead, we deliberately tried to remove from the catalog galaxies with morphologies clearly disturbed due to mergers or tidal interactions, still retaining and flagging the most doubtful cases where either gas stripping or tidal forces, or both, might be at work. In fact, the eventual presence of tidal forces does not exclude the possibility that also gas stripping mechanisms, such as ram pressure, are at work, as it is sometimes observed (e.g., NGC 4654 in Virgo, Vollmer 2003). Thus, the reader should be aware that the catalog comprises galaxies for which the optical morphology alone is not sufficient to identify beyond any doubt the physical origin of the stripping, that can be pinpointed only by gas-sensitive follow-up studies. Only subsequent studies, in fact, will be able to discriminate between different processes that can give origin to similar morphological features, such as harassment (especially in clusters, Moore et al. 1996) and minor mergers (also in groups and low density environments, Bournaud et al. 2004; Cox et al. 2008; Hopkins et al. 2009; Lotz et al. 2010a, 2010b).

It is important to keep in mind that the "JClass" depends not only on the intrinsically stronger or weaker evidence for stripping signatures, but also on the galaxy orientation with respect to the line of sight, the galaxy size (number of pixels) and the signal-to-noise of the images, thus it is only crudely indicative of the effective degree of surrounding debris.

3.1. Galaxy Properties

The galaxy current SFR, stellar mass and absolute magnitudes were derived applying our spectrophotometric tool SINOPSIS to the available optical spectroscopy, as described in Fritz et al. (2011) for WINGS, A. Moretti et al. (2016, in preparation) for OMEGAWINGS and Poggianti et al. (2013) for PM2GC. The model performs a non-parametric full spectral fitting of the continuum shape and of the main emission and absorption lines, deriving a star formation history. The ongoing SFR is constrained from the fluxes of the emission lines and the blue part of the spectrum, and dust extinction is taken into

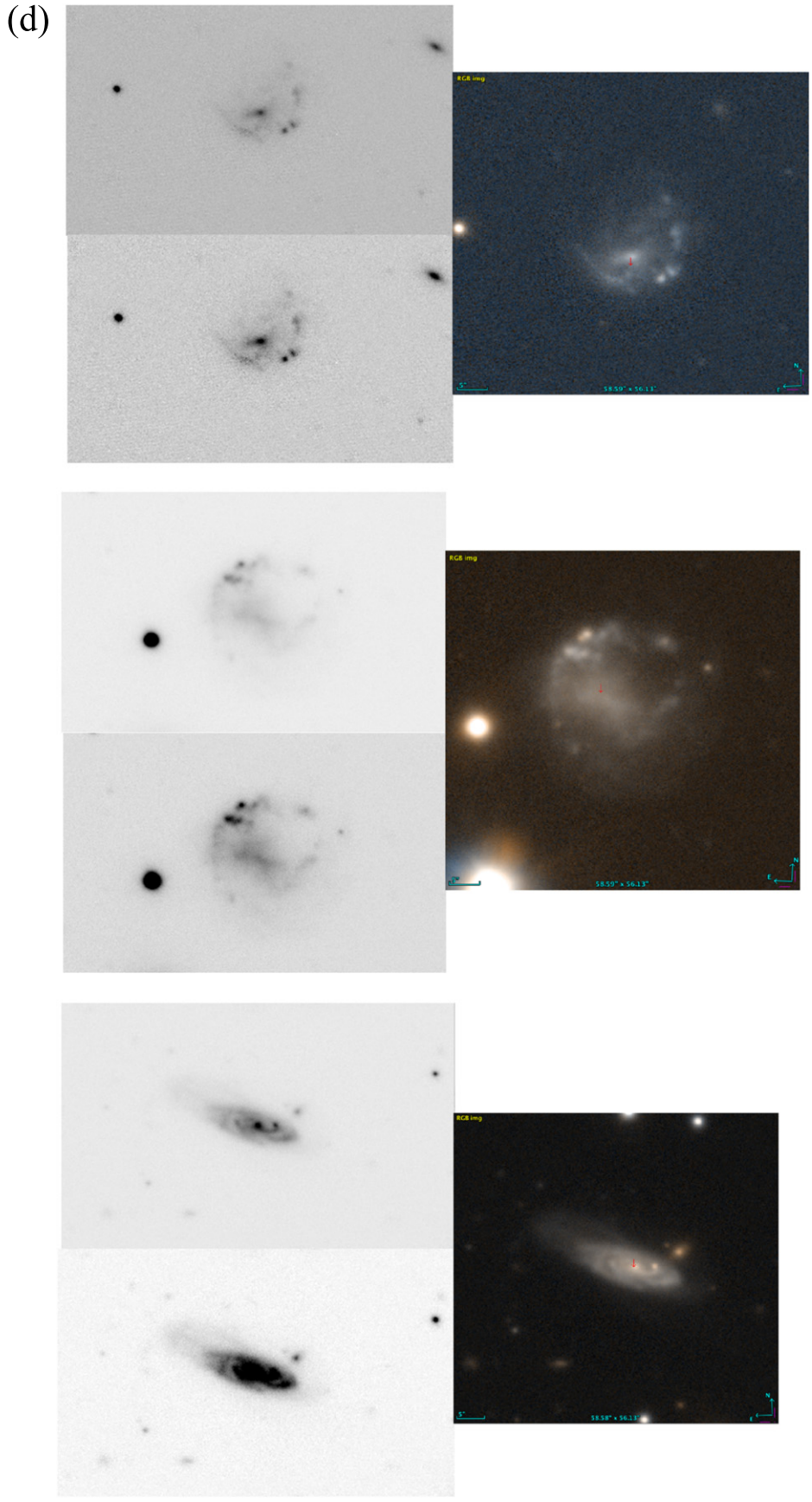

Figure 1. (Continued.)

(e)

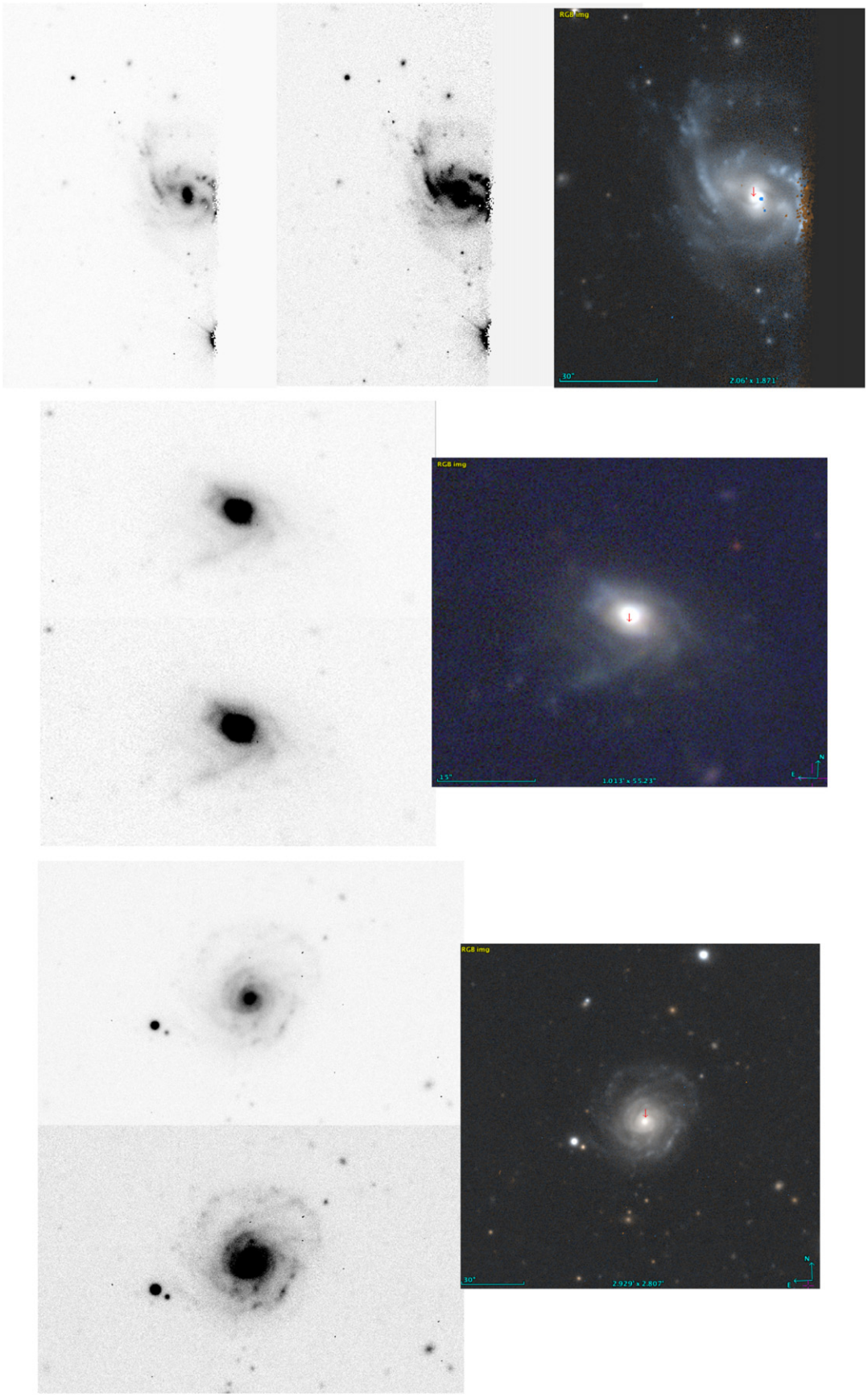

Figure 1. (Continued.)

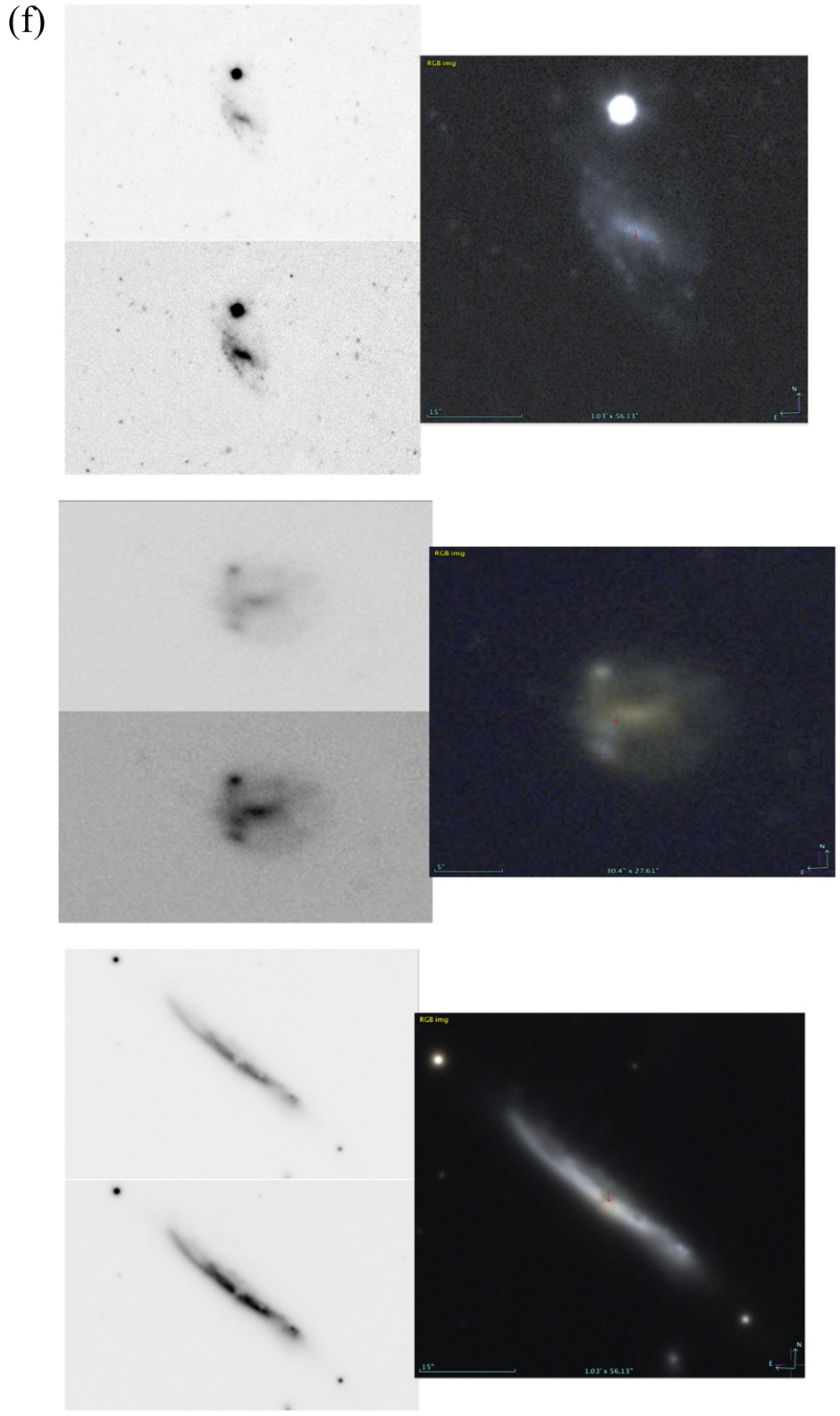

Figure 1. (Continued.)

account (see Fritz et al. 2007, 2011 for details). Being obtained from multifiber spectroscopy, the SFR estimate refers to the central region of galaxies that is covered by the fiber (that has a diameter of 2.1 arcsec, covering the central 1.7–2.8 kpc at the WINGS redshifts), and is then extrapolated to a total SFR value assuming the same mass-to-light ratio within and outside of the fiber. The mean correction factor is 6, with a standard deviation of 4.8.

Galaxies were assigned a spectral type on the basis of the strength of their main emission and absorption lines, as done in

Table 2
Number of Stripping Candidates

Sample	$N_{stripping}$	N_5	N_4	N_3	N_2	N_1	N_z	N_{mem}	$N_{other\text{-}mem}$	$N_{non\text{-}mem}$
OMEGAWINGS	211	8	19	48	66	70	158	107	7	44
WINGS	133	2	2	19	49	61	78	56	0	22
PM2GC	75	0	3	6	28	38	75	⋯	⋯	⋯
Total	419	10	24	73	143	169	308	nd	nd	nd

Note. Columns: (1) Sample, (2) number of candidates, (3,4,5,6,7) number of JClass=5,4,3,2,1 candidates, (8) number of candidates with a known spectroscopic redshift, (9) number of spectroscopic cluster members, (10) number of spectroscopic members of other known structures in the fore/background of the main cluster, (11) number of galaxies with redshift that belong neither to the main cluster nor to other fore/background known structures.

Fritz et al. (2014). In the following we distinguish between "star-forming galaxies" (all those with emission lines) and "post-starburst" (k+a) and "passive" (k) galaxies that lack emission lines and have a strong and a weak Hδ line in absorption, respectively. The post-starburst signature testifies the presence of recent SF activity that ended sometime during the last ∼1 Gyr, while k galaxies are those that have been devoid of any SF for a longer time (Poggianti et al. 1999, Fritz et al. 2014).

Morphological classifications are available for WINGS (Fasano et al. 2012) and PM2GC galaxies (Calvi et al. 2012).[10] They were obtained with MORPHOT, an automated tool designed to reproduce as closely as possible the visual classifications (Fasano et al. 2012). MORPHOT adds to the classical CAS (concentration/asymmetry/clumpiness) parameters a set of additional indicators derived from digital imaging of galaxies and has been proved to give an uncertainty similar to that of eyeball estimates. It uses a combination of a Neural Network and a Maximum Likelihood technique assigning a morphological class T with a scale resembling the Revised Hubble Type classification, for which $T = -5$ = elliptical, -2 = S0, 1 = Sa, 3 = Sb, 5 = Sc, 7 = Sd, 9 = Sm.

4. ATLAS

Table 2 presents the number of candidates in the three samples, globally and for each JClass separately, as well as the number of candidates with an available spectroscopic redshift. In total, our sample comprises 419 candidates, of which 10 of JClass=5, 24 of JClass = 4, 73 of JClass = 3, 143 of JClass = 2 and 169 of JClass = 1.

Figures 1–5 present illustrative examples of OMEGAWINGS, WINGS and PM2GC candidates. We present a single filter image with two different cuts, as well as a color-composite image.

For OMEGAWINGS, in Figure 1 we show all JClass=5 galaxies, six JClass = 4 candidates and one example of each of JClass = 3,2 and 1. For WINGS, we show examples of each JClass in Figure 2. Finally, for PM2GC we show two examples for each JClass from 4 to 1 in Figure 3 (no JClass=5 candidate is present in the PM2GC).

The complete atlas with all images in pdf format is available in the online version of the paper, where we give both the rgb image and two individual filter images if more than one filter is available (for OMEGAWINGS and WINGS). For spectroscopically confirmed cluster members, the red line in the single filter images points in the direction of the cluster X-ray center. In addition, for the JClass = 1 OMEGAWINGS candidates, which are the hardest to visualize, we provide an additional pdf single-filter image with different cuts. Since the appearance of the pdf figures strongly depends on the screen or printer used and this can make it hard to visualize the features of interest, we also provide OMEGAWINGS cutouts images of each candidate in fits format to allow the reader to display each image with the most appropriate cuts for her/his screen/printer. For WINGS, all the images are public through the VO, as described in detail in Moretti et al. (2014). For the PM2GC, all the images are made public by the Millennium Galaxy Catalog team (http://www.eso.org/~jliske/mgc/).

Tables 3 and 4 contain the catalogs of all candidates. These tables list positions on the sky, JClass and relative comments, redshift when available and the redshift source. For OMEGAWINGS and WINGS, the eventual membership to the cluster and the type of image and filter used are also given. The comments include some notes on the several peculiar morphologies we have encountered, for example describe shapes similar to a "croissant," or to a bicycle's "handlebar," or if a galaxy looks comet-like/tadpole.

Whenever a candidate could be suspected to be tidally interacting, due to presence of a nearby galaxy and/or to a possibly winding morphology of the tails, or to have possibly experienced a minor merger, this possibility has been recorded in the comments as "tidal." Similarly, we have recorded whether the morphological signature might resemble the one expected from the harassment process. About 20% of candidates in OMEGAWINGS and 40% in WINGS and PM2GC have been flagged as possibly tidal, interacting, merging or harassed. Instead, as explained in Section 3, we tried not to include in the sample galaxies with clear evidence for a tidal interaction or a merger.

This is by far the largest existing sample of stripping candidates, with 344 galaxies in OMEGAWINGS+WINGS and 75 in the PM2GC sample, and a spectroscopic redshift for ∼70% of them. They are homogeneously selected and cover a wide range of environments, that will be discussed in the following section.

5. LOCATION OF STRIPPING CANDIDATES

Out of the 158 + 78 OMEGAWINGS+WINGS candidates with a spectroscopic redshift, 107 + 56 (∼70%) are cluster members.

Our clusters cover a wide range of σ and L_X (thus cluster mass), but the number of candidates per cluster (spectroscopic members plus possible members because without a redshift) does not depend on either of these observables, nor on redshift in our narrow z range (Figure 4). This result does not change if

[10] The morphological analysis of the OMEGACAM images is ongoing, therefore, for now, for the OMEGAWINGS clusters morphologies are only available on the smaller area covered by WINGS.

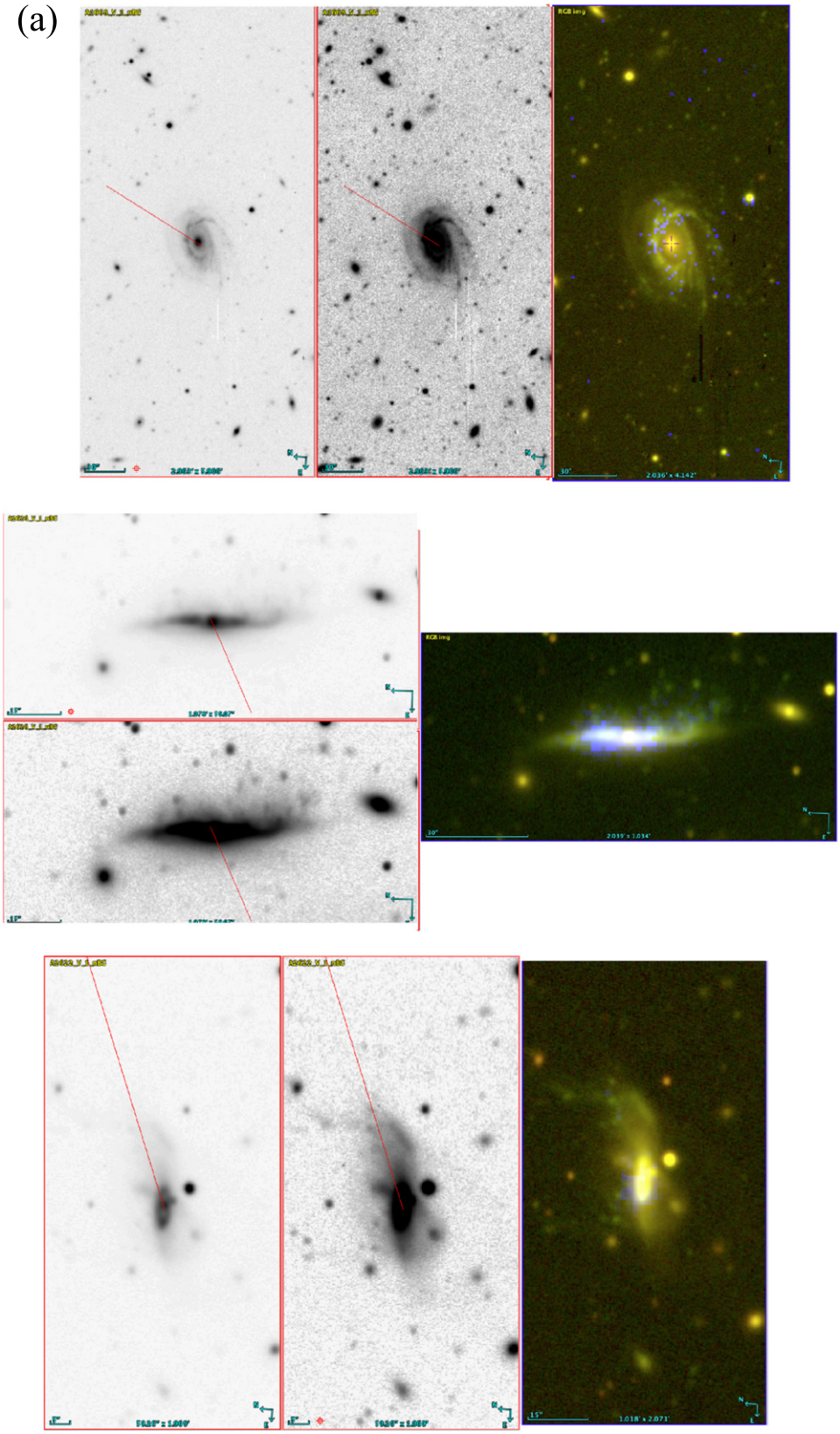

Figure 2. (a) Examples of JClass=5 (top and middle) and JClass = 4 (bottom) WINGS candidates. (b) Examples of JClass=3 (top), JClass=2 (middle) and JClass=1 (bottom) WINGS candidates. Left and center: B-band image with two different stretches. Right: color-composite image.

(The complete figure set (133 images) is available.)

(b)

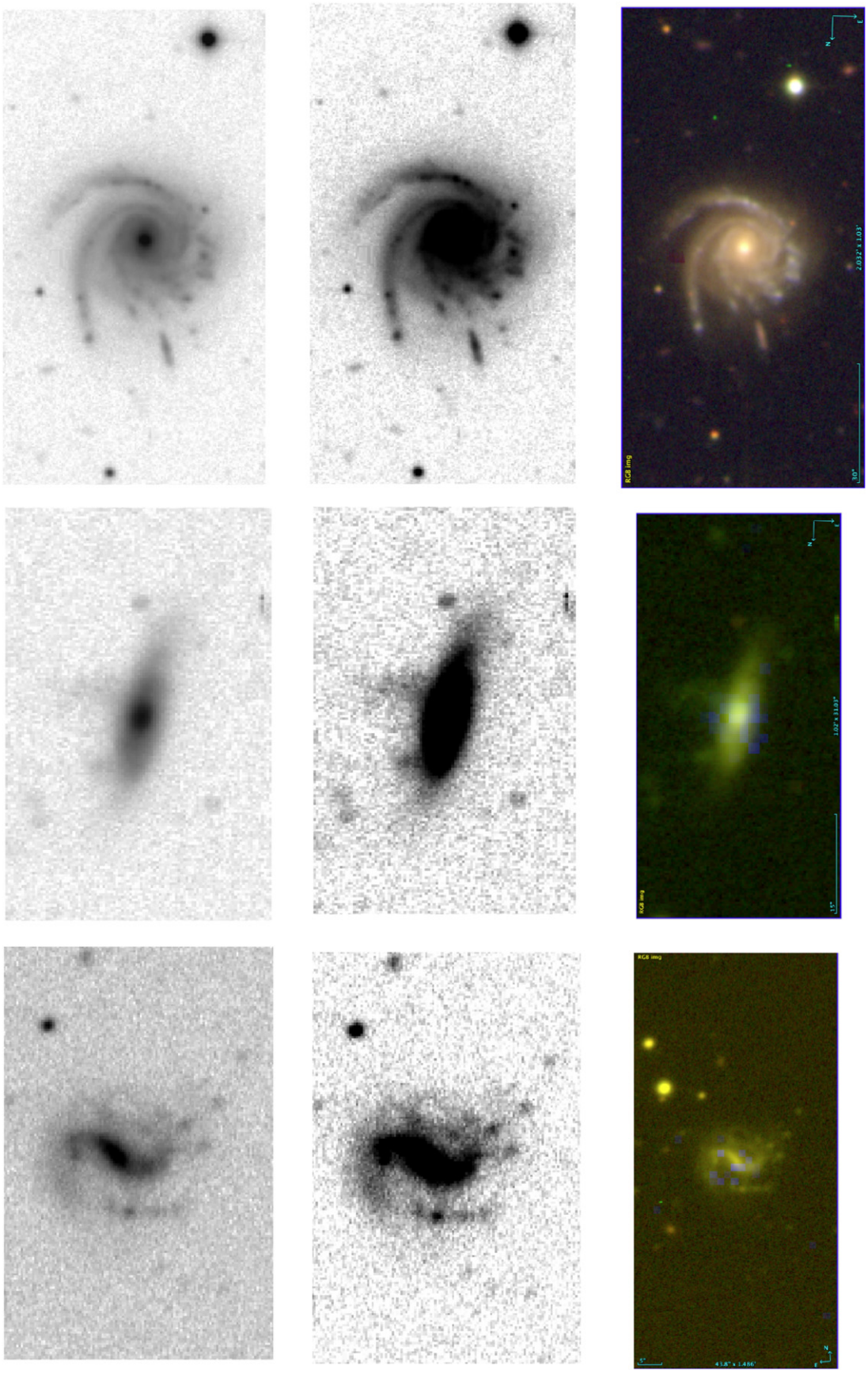

Figure 2. (Continued.)

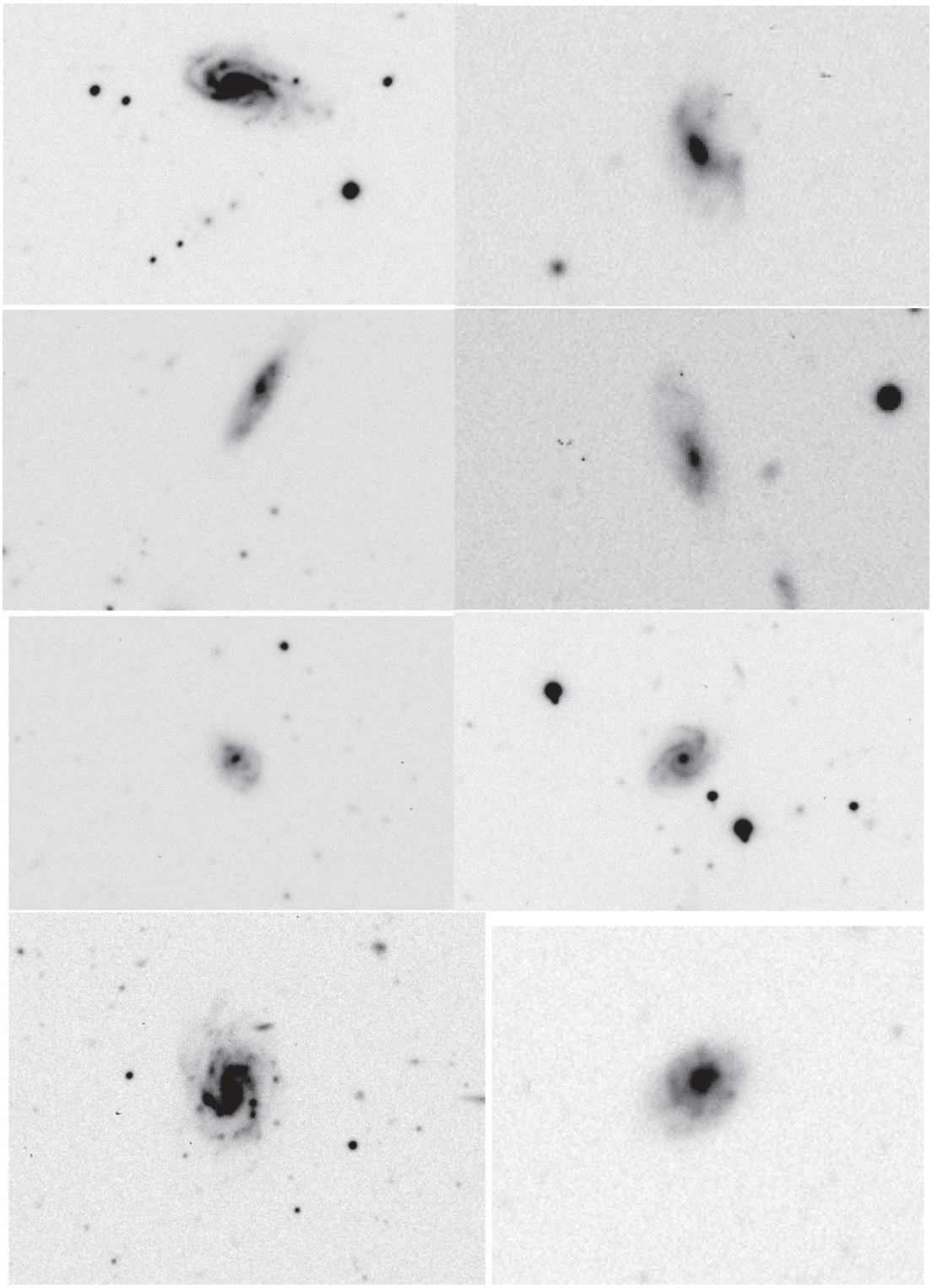

Figure 3. Two examples of each JClass = 4, 3, 2 and 1 (from top to bottom) PM2GC stripping candidates. They belong to all types of environmental conditions found in the PM2GC, from groups to single systems.

(The complete figure set (75 images) is available.)

we only consider stripping candidates that are spectroscopically confirmed members. Also considering only the number of most secure candidates (JClass 3,4,5), there is no sign of a correlation with σ or L_X. The independence of the number of candidates should be taken with caution for two reasons: the incomplete spectroscopic membership, and the fact that we are observing a fixed area on the sky (the OMEGACAM field), that corresponds to different fractions of the cluster virial radius.

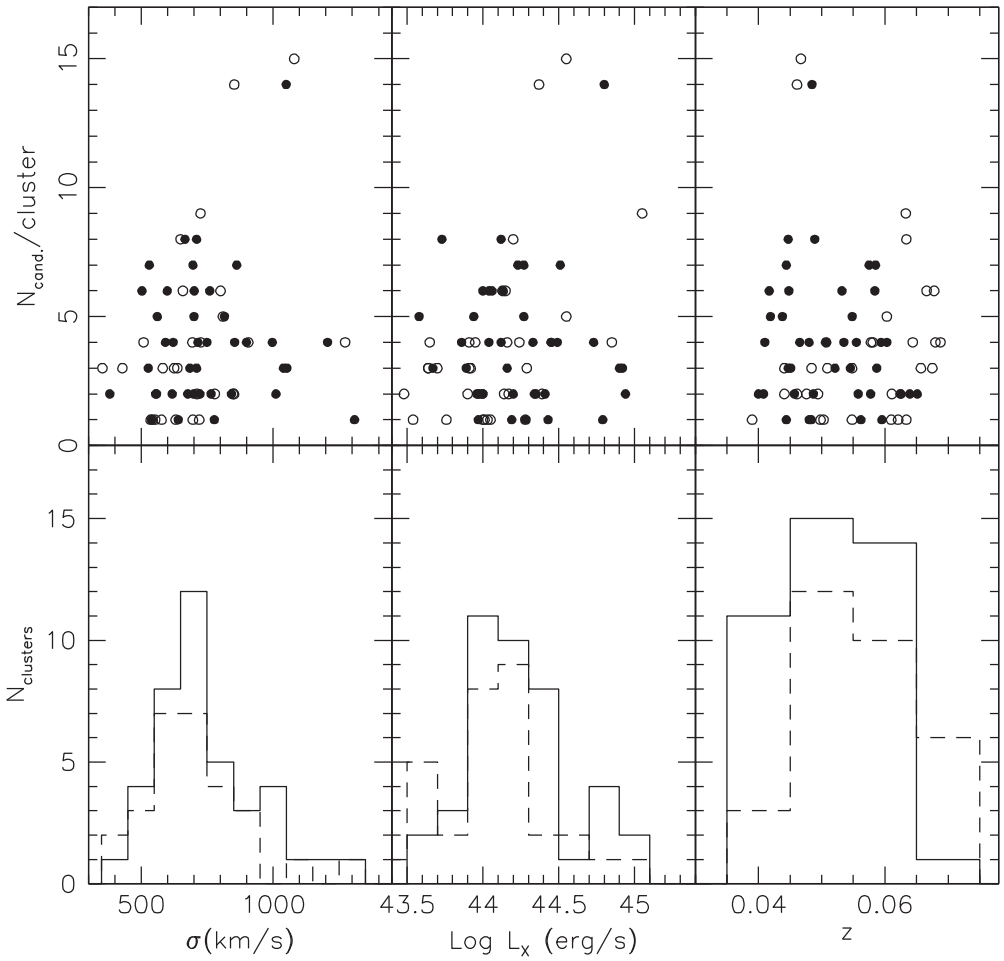

Figure 4. Top Number of stripping candidates per cluster (members and possibly members, because without redshift) as a function of cluster σ, L_X and z. Bottom Distribution of σ, L_X and z of clusters with candidates. Filled points and solid histogram OMEGAWINGS, empty points and dashed histogram WINGS.

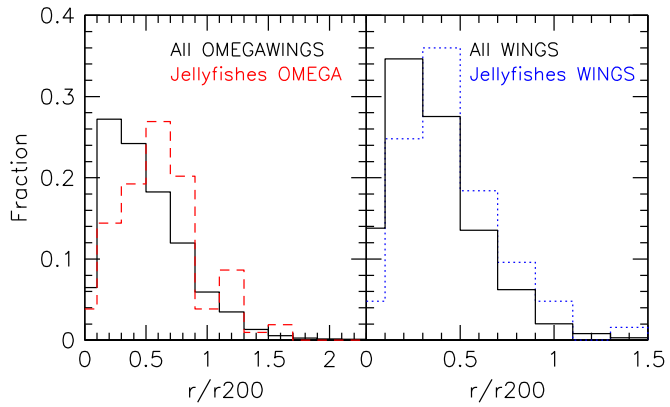

Figure 5. Radial distribution in units of R_{200} of all OMEGAWINGS cluster members (left, black histogram) plus OMEGAWINGS stripping candidates (left, dashed red histogram), and all WINGS cluster members (right, black histogram) plus WINGS candidates (right, dotted blue histogram).

Nonetheless, it is striking that stripping candidates are found in all clusters inspected and, even more, that they can be present in large numbers even in 500 km s^{-1}, low-mass clusters. Moreover, the strength of the stripping signatures is not correlated with σ or L_X either. In particular, the fraction of JClass = 3,4,5 candidates with respect to all candidates is not significantly correlated with σ or L_X. This raises the question what is the minimum halo mass that can trigger the stripping phenomenon, which we will address in the following with the PM2GC sample.

While the average number of candidates per cluster that are members or could be members (have no redshift) is 4.6 ± 0.7, this number rises to 6.1 ± 0.5 in clusters of the Shapley supercluster, suggesting the supercluster environment could be particularly favorable for stripping phenomena. This is consistent with the hypothesis that ram pressure effects are enhanced wherever the merging of structures produces shocks and strong temperature gradients in the IGM (Owers et al. 2012; Vijayaraghavan & Ricker 2013). There are smaller superclusters and cluster mergers in our sample, and the relation with large scale structure and cluster substructure will be explored in forthcoming papers.

Candidates that are cluster members are observed at all clustercentric radii, though their distribution is skewed toward larger radii than the global population of members (Figure 5), as it is expected for a population of mainly late-type galaxies. Here and throughout the paper clustercentric radii are projected radii on the plane of the sky, in units of R_{200}, measured from the Brightest Cluster Galaxy. We note that the OmegaCAM field of view probes between ~1.2 and 2.4 times the cluster virial radius R_{200}, depending on cluster redshift and extension, thus in the left panel of Figure 5 the coverage is complete for all clusters only out to $r/r_{200} = 1.2$.

For about 80% of the cluster member candidates, it is possible to identify one main direction of the stripped material

Table 3
OMEGAWINGS and WINGS Stripping Candidates

ID	Cluster	Image	Band	R.A.	Decl.	JClass	Comments	Memb.	z	Source z
JO1	A1069	O	V	160.4327677	−8.4198195	1	disturbed	2	0.05765	1
JO2	A1069	O	V	160.1087159	−8.2662606	2	⋯	−1	⋯	⋯
JO3	A1069	O	V	160.1466322	−8.4630044	2	⋯	2	0.15894	1
JO4	A1069	O	V	159.9728672	−8.9068175	2	⋯	2	0.05541	1
JO5	A1069	O	V	160.334885	−8.8961043	3	⋯	1	0.06484	1
JO6	A119	W	B	14.2420529	−1.2992219	1	tidal	0	0.07326	1
JO7	A119	O	B	13.806715	−1.0760668	2	⋯	1	0.04762	3
JO8	A119	O	B	14.4873539	−1.3355165	2	⋯	−1	⋯	⋯
JW1	A133	W	B	15.5496061	−21.6593958	3	tidal	−1	⋯	⋯
JW2	A133	W	B	15.7618501	−21.6613987	3	warping	−1	⋯	⋯
JW3	A133	W	B	15.8219828	−21.7460609	2	⋯	1	0.0529	2
JW4	A133	W	B	15.4267328	−21.9509146	1	⋯	−1	⋯	⋯
JW5	A133	W	B	15.5625195	−22.0113691	1	⋯	1	0.0515	2
JW6	A311	W	B	32.2268083	19.7558379	1	tidal	−1	⋯	⋯
JW7	A311	W	B	32.0011882	19.698108	2	tidal	−1	⋯	⋯

Note. Columns: (1) ID: JO for OMEGAWINGS clusters and JW for WINGS clusters (2) Cluster (3) Image inspected: O = OMEGAWINGS (OmegaCAM) or W = WINGS (INT or 2.2 m) (4) Band used (5) R.A. (J2000) (6) decl. (J2000) (7) JClass: from 5 (strongest) to 1 (weakest) (8) comments (9) Cluster membership: 1 = member, 0 = non member, 2 = member of structure along the line of sight, −1 = redshift unknown (10) Redshift (11) Source of redshift: 1 = WINGS (Cava et al. 2009) or OMEGAWINGS (A. Moretti et al. 2016, in preparation), 2 = NED, 3 = SDSS, 4 = average NED and SDSS.

(This table is available in its entirety in machine-readable form.)

on the plane of the sky. For these, the "tentacles" or main tail point away from the cluster center in ∼35% of the cases, point toward the cluster center in ∼13% of the cases, and form an angle (not 0, nor 180°) with respect to the cluster center in ∼52% of the cases. This non-alignment between the tails and the direction to the cluster center can originate from non radial orbits, but also if the stripping is caused by encounters with IGM substructures and shocks.

Seven ($4 \pm 2\%$) of the OMEGAWINGS candidates that are not members can be assigned to other structures (clusters or groups) along the line of sight, in the foreground or background of the main WINGS cluster in that field (flag = 2 in Column 9 of Table 3). Some of the flag = 2 candidates belong to groups with $\sigma < 400\,\mathrm{km\,s^{-1}}$. The best examples are the two candidates in the field of A1069 ($z = 0.0651$) that belong to a $\sigma = 372 \pm 84\,\mathrm{km\ s^{-1}}$ structure at $z \sim 0.56$ (A. Moretti et al. 2016, in preparation).

Finally, there is not sufficient spectroscopic information to characterize the environment of the 44 remaining candidates with redshifts ($28 \pm 4\%$ of all candidates with redshift) belonging neither to the main cluster nor to other foreground known structures (flag = 0 in Table 3).

However, the group environment is better investigated with the PM2GC sample.[11] The mass distribution of halos hosting stripping candidates is shown in Figure 6. All PM2GC candidates are found in halos with masses 10^{11}–$10^{14} M_{\odot}$.[12] This is somewhat surprising, as the stripping phenomenon has always been associated with ram pressure stripping in the past, and the latter is often believed to be effective only in massive clusters with a hot and dense intracluster medium. However, evidence for ram pressure effects in groups is present in the literature (e.g., Rasmussen et al. 2006; Sengupta & Balasubramanyam 2006) and there is at least one known case of ram pressure stripping in a galaxy pair, where NGC4485 is stripped during its passage through the extended H I distribution of its companion, NGC4490 (Clemens et al. 2000). The PM2GC sample has a considerable number of stripping candidates with features as convincing as those in clusters (JClass = 4 and 3, see Figure 3 and full sample online), and even they (as all candidates) are clearly *not* located in a cluster.

This is an interesting result, suggesting either that (a) ram pressure stripping can be efficient in lower mass halos than commonly believed (e.g., Clemens et al. 2000), or (b) there are other types of physical processes that work in groups (and perhaps clusters as well) that produce similar debris morphologies and similar signatures for stripped gas. In groups and low-mass halos in general, the most likely candidates for such processes are tidal interactions and minor or major mergers. We reiterate that 40% of the PM2GC stripping candidates have been flagged as possibly tidal, interacting, undergoing merging (no harassment candidates have been found in the PM2GC). Studying in detail a sample of stripping candidates in groups will therefore be crucial to understand the impact of gas stripping processes on galaxy evolution in general. An ongoing program of this kind based on the sample presented in this paper is described in Section 7.

6. MORPHOLOGIES, SF, COLORS AND MASSES

The distribution of morphological types for the three samples[13] of stripping candidates is shown in Figure 7. The great majority of them are disk galaxies of types between Sab

[11] The MGC stripe does not contain any X-ray cluster at $z = 0.04$–0.07 at the X-ray flux limit of the WINGS selection (BCS+eBCS +XBACS samples, Ebeling et al. 1996, 1998, 2000), except A957x which has three identified stripping candidates. Unfortunately, the MGC area covers only a fraction of the cluster, and the three candidates are outside of the PM2GC field.

[12] Their hosting systems can be "groups," binary or even single systems according to the PM2GC classification (Section 2.2). We stress that such environmental definitions depend on the criteria chosen, which are necessarily arbitrary at some level, and therefore are only roughly indicative of the richness of the host system.

[13] As written in Section 3.1, morphological classifications are available only for WINGS and PM2GC, while the analysis is still ongoing for OMEGAWINGS. The OMEGAWINGS morphologies in Figure 7 are those taken from the WINGS images of OMEGAWINGS clusters.

Table 4
PM2GC Stripping Candidates

MGC ID	R.A.	Decl.	JClass	z	Comments
648	150.3656	0.15526	1	0.06646	⋯
669	150.50264	0.17896	1	0.04648	⋯
738	150.36314	−0.04522	1	0.06571	⋯
954	150.51414	−0.21385	2	0.0452	tidal
1158	151.05859	0.26304	1	0.0671	⋯
1241	150.82014	−0.00452	1	0.06571	⋯
3425	153.00465	−0.08858	1	0.06978	⋯
3481	152.71695	−0.13429	1	0.06882	⋯
3924	153.24818	−0.07149	1	0.06285	⋯
3984	153.52425	−0.12731	4	0.04649	⋯
4686	153.89871	−0.26982	2	0.06341	tidal
4946	154.6284	0.08481	2	0.06235	⋯
5055	154.53592	−0.08383	2	0.06111	⋯
5215	154.24265	−0.248	2	0.06296	⋯
5789	155.41989	0.21857	1	0.05846	⋯
7591	156.81654	−0.20765	1	0.05633	tidal
8694	158.45477	0.16144	1	0.05557	interaction
8721	158.53624	0.00101	3	0.065	⋯
8770	158.53114	−0.04816	1	0.06486	tidal
9223	158.97345	−0.05658	1	0.0587	tidal
11695	161.56158	0.05042	4	0.0466	merger
12660	162.84444	0.2626	1	0.04004	prob tidal
13024	162.88519	−0.28004	1	0.05635	⋯
13384	163.26303	−0.22522	1	0.05133	⋯
13515	163.95135	0.22002	2	0.04109	tidal
14272	164.21922	0.02732	1	0.05488	⋯
15672	166.44359	0.23992	1	0.06717	⋯
17048	168.15927	0.13376	3	0.0489	tidal
17873	168.15373	0.0109	1	0.05516	tidal
17945	168.86038	0.2699	1	0.04402	⋯
18060	168.74698	−0.01211	1	0.04302	⋯
19313	169.72412	0.02301	1	0.05846	⋯
19482	170.63046	−0.01728	1	0.04078	⋯
20159	171.09225	−0.27661	2	0.04906	⋯
20769	171.82335	0.19009	1	0.0491	⋯
20883	171.93929	−0.1212	2	0.06175	⋯
20925	172.13615	−0.17166	2	0.06421	⋯
24049	175.8248	−0.18163	1	0.05571	⋯
24069	176.01851	−0.21116	1	0.04844	tidal
25500	177.90108	6.0E-4	2	0.0605	⋯
26189	178.56143	0.01557	1	0.05636	⋯
26597	179.07112	0.05586	1	0.06486	tidal
29909	182.80855	0.18497	1	0.06299	tidal
30102	182.64824	−0.17155	1	0.05052	tidal
30802	183.97357	0.08151	1	0.04021	⋯
31663	184.7652	0.0811	1	0.06818	tidal
36727	190.8569	−0.08998	1	0.04782	⋯
40457	195.38736	−0.08069	3	0.06799	⋯
42932	197.68634	0.03204	1	0.04079	⋯
44092	199.55598	−0.14834	2	0.04877	tidal
44601	199.73911	−0.19856	1	0.05426	⋯
45094	200.17049	−0.20287	1	0.0467	tidal
45479	200.8947	−0.13107	1	0.05159	⋯
45979	201.23416	−0.1341	2	0.0666	tidal
48127	204.03214	0.2167	1	0.06204	⋯
48157	204.00653	0.26251	1	0.06156	⋯
57255	212.15759	−0.22513	1	0.05209	⋯
57486	212.89355	0.16627	1	0.05275	⋯
59348	214.51141	0.13088	1	0.05451	⋯
59391	214.60939	0.16948	1	0.05324	⋯
59597	214.42107	−0.14422	2	0.04964	⋯
60136	215.06152	−0.07929	1	0.05273	⋯
60151	214.69313	−0.08358	2	0.05329	tidal/ superposition?
61980	216.28696	−0.12431	1	0.05463	tidal
62927	217.67888	0.25342	3	0.05493	prob merger
63504	218.13986	0.10742	1	0.0554	⋯
63661	218.09081	0.17823	2	0.05479	⋯
63692	218.00017	0.08422	1	0.0557	⋯
63947	217.75774	−0.18262	2	0.05574	⋯
90126	163.0394	0.01269	2	0.04057	⋯
95080	198.03625	−0.23903	1	0.04049	⋯
96244	214.64769	0.15756	4	0.05303	⋯
96248	217.4342	0.08132	1	0.05469	⋯
96328	214.13489	0.07133	2	0.05259	⋯
96949	178.54276	0.13871	3	0.05014	interaction/ projection

Note. Columns: (1) ID (2) MGC ID (3) R.A. (J2000) (4) decl. (J2000) (5) JClass: from 5 (strongest) to 1 (weakest) (6) MGC redshift (7) comments.
(This table is available in machine-readable form.)

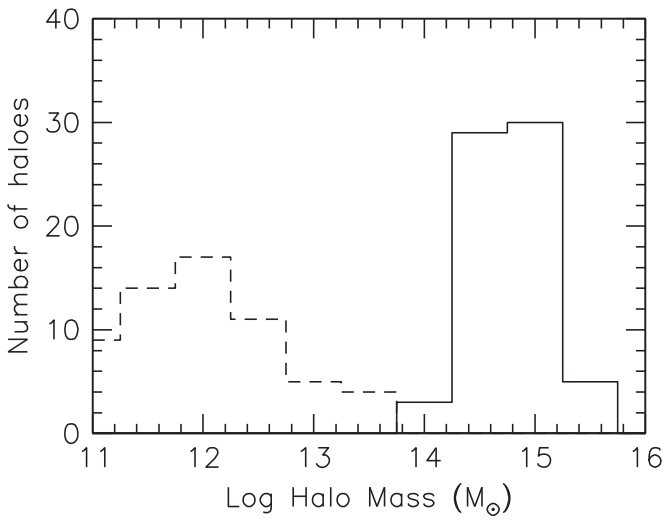

Figure 6. OMEGAWINGS+WINGS (solid histogram) and PM2GC (dashed histogram) mass distribution of halos hosting stripping candidates. All JClasses are included.

and Sc, with a tail of earlier and later types. According to a Kolmogorov–Smirnov (KS) test, while the OMEGAWINGS and WINGS distributions could be drawn from the same parent population, the PM2GC distribution differs significantly from the other two, with a KS probability greater than 99.8% and 99.999% versus OMEGAWINGS and WINGS, respectively.

We visually checked all candidates classified by MORPHOT as ellipticals or S0s and, indeed, except for the stripping signatures, they appear to have early-type morphologies. When available, their spectra always show emission lines.

The bottom panel of Figure 7 shows the morphological distributions of the whole parent samples of galaxies in WINGS and PM2GC. They exhibit a much more prominent early-type population and are radically different from the morphological distributions of stripping candidates: the KS test can rule out that each stripping candidates distribution is drawn from its parent catalog with >99.999% probability.

The SFR-stellar mass relation of candidates is contrasted with that of all star-forming galaxies in Figure 8 for

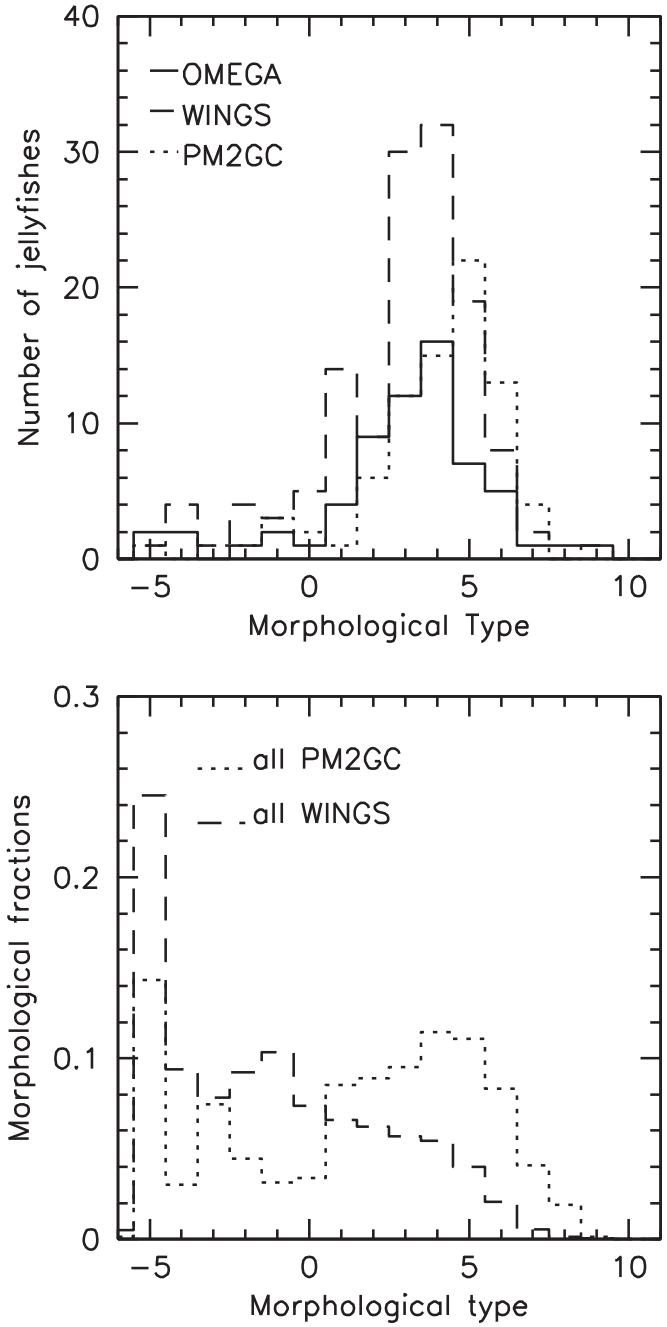

Figure 7. Top panel. Distribution of morphological types for stripping candidates in OMEGAWINGS (solid histogram), WINGS (dashed histogram) and PM2GC (dotted histogram). The main morphological types are: −5 = elliptical, −2 = S0, 1 = Sa, 2 = Sab, 3 = Sb, 4 = Sbc, 5 = Sc, 7 = Sd, 9 = Sm. Bottom panel. As in top panel, distribution of morphological types for all galaxies in the WINGS and PM2GC parent galaxy samples. sample

OMEGAWINGS+WINGS and PM2GC separately. Stripping candidates tend to be located above the best fit to the relation, indicating a SFR excess with respect to non-candidate galaxies of the same mass. To make sure that this conclusion is not influenced by contamination of tidally disturbed galaxies, we plot non-tidal and possibly tidal candidates with different symbols. Even considering only the most secure candidates (non-tidal, of JClass 3,4,5), the SFR excess is clearly visible in the plot.

If we define the fraction of secure stripping candidates as the ratio between the number of candidates of JClass $\geqslant 3$ and the total number of galaxies with a SFR $> 0.1\ M_{\odot}\ \mathrm{yr}^{-1}$ that can be located on the SFR-Mass diagram above the mass completeness limit of each sample, this fraction is about 2% for both OMEGAWINGS and PM2GC. This gives a rough indication of the frequency of the most secure stripping candidates within the global galaxy population.

The SFR excess, measured as distance from the fit at fixed mass, is plotted in the bottom panels. On average, the SFR of stripping candidates is enhanced by a factor 2.3/1.7 in OMEGAWINGS candidates of JClasses (3,4,5)/(1,2), respectively (red and green points), and a factor ∼8.6/1.7 in PM2GC, at masses above the mass completeness limit.[14] Comparing the least square linear fit of the SFR-mass relations of stripping candidates with that of all other galaxies (keeping fixed the slope shown in Figure 8), the offset is 2.5 times the errorbar on the intercept, thus the excess can be considered significant approximately at the 98.7% level.

The individual SF estimates are highly uncertain as they are obtained extrapolating the SF rate measured within the central galaxy regions covered by the fiber to a total value assuming a constant mass-to-light ratio (see Section 3). To assess their reliability as integrated SFR estimates, we have derived SFRs from W4 fluxes from the ALLWISE Source Catalog (Wright et al. 2010; Mainzer et al. 2011) using Equation (14) in Rieke et al. (2009) and rejecting those sources that are flagged as spurious detections or image artifacts. Comparing the *WISE*-based SFR-mass relation of candidates and non candidates (not shown) in OMEGAWINGS+WINGS, we derive the integrated SFR excess (dashed lines in the bottom left panel of Figure 8). Due to the relatively high SFR detection limit of *WISE* (∼1 $M_{\odot}\ \mathrm{yr}^{-1}$ at the WINGS redshifts) the statistics are poor, but qualitatively the *WISE* estimates confirm our spectral modeling findings: on average, using *WISE*, the SFR of OMEGAWINGS +WINGS stripping candidates is enhanced by a factor 1.8/1.7 for JClasses (3,4,5)/(1,2).

Considering the spectral classes, the great majority of stripping candidates have emission lines. Only 3 out of 85 galaxies with an assigned spectral type in OMEGAWINGS are k + a's, and only 2 are k's. Similar trends are found in WINGS (no k+a, 2 k's out of 27) and PM2GC (1 k+a and 6 k's out of 67). The lack a significant ongoing SFR in k + a's and k's candidates, not just in the galaxy center but throughout the galaxy, is confirmed by the *WISE* data, that find no detection or very weak SFR upper limits ($\ll 1 M_{\odot}\ \mathrm{yr}^{-1}$).

All k+a and k stripping candidates have weak stripping signatures (mostly JClass 1 or 2). This might indicate that, generally, the phase when the stripping is most evident in the optical image corresponds to an early stage of the process, when the galaxy SFR is enhanced, probably before being quenched in later phases. Alternatively, it is possible that the morphological disturbance we see in the k+a/k galaxies arises from a different process, not related to stripping.

The rest frame U–V-stellar mass relation is shown in Figure 9 for OMEGAWINGS+WINGS.[15] Stripping candidates are among the bluest galaxies of their mass, and are mostly

[14] The mass limits are computed as the mass of the reddest galaxy at the highest redshift at the spectroscopic magnitude limit in each sample, $\log M/M_{\odot} = 9.8$ for WINGS and 10.2 for PM2GC (see Vulcani et al. 2011 and Calvi et al. 2013 for details).

[15] The color is not available for PM2GC.

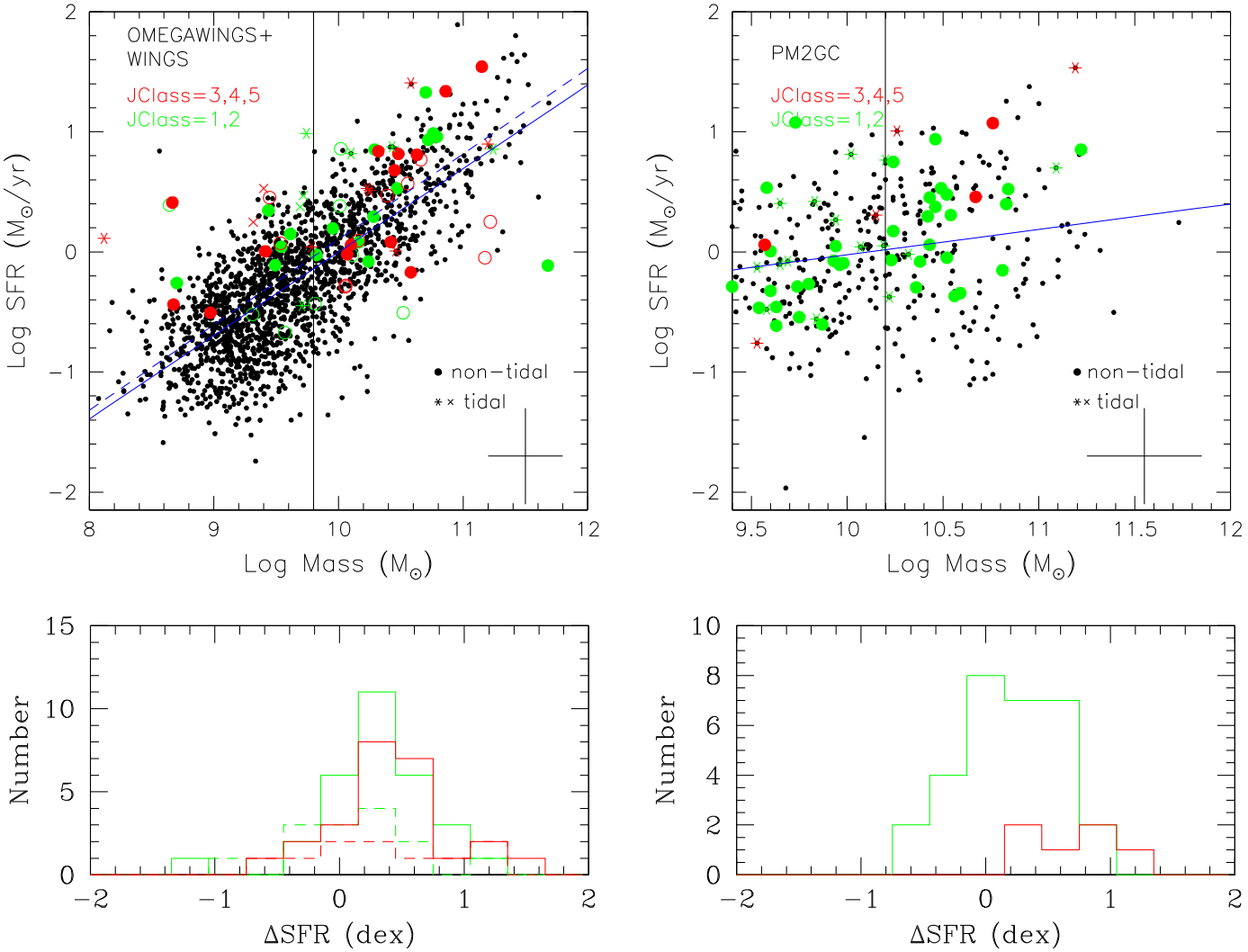

Figure 8. Top SFR-Mass relation for stripping candidates and all other galaxies in OMEGAWINGS+WINGS (left) and PM2GC (right). JClass = 1 and 2 in green, 3, 4 and 5 in red. Filled circles are non-tidal OMEGAWINGS and PM2GC, stars are possibly tidal OMEGAWINGS and PM2GC. Empty circles are non-tidal WINGS, crosses are possibly tidal WINGS. The blue line is the least square fit of cluster (solid line) and WINGS field (dashed line) galaxies in the left panel, and of all PM2GC galaxies in the right panel. The vertical lines indicate the mass completeness limit of each survey. The uncertainty on the SFR can be estimated as the scatter obtained using independent SFR estimates of galaxies in our sample. Comparing with SDSS (P2MGC) and *WISE* (OMEGAWINGS) values, this uncertainty turns out to be ∼0.4 dex and is shown in the right bottom corner of the plot. Bottom Distribution of SFR excess with respect to the best fit SFR-Mass relation for OMEGAWINGS (left) and PM2GC (right). JClass = 1 and 2 in green, 3, 4 and 5 in red. In the left panel, solid lines are for the model SFR estimates, dashed histograms for *WISE* SFR estimates (see text).

located in the blue cloud, but they could not be singled out simply on their location in the color–mass diagram. Their color does not depend on JClass.

Finally, our stripping candidates cover a wide range in stellar mass, from log $M/M_{\odot} < 9$ to >11.5, and there is no correlation between mass and JClass. Their stellar mass distribution, both in clusters and in the field, is similar to that of the global galaxy population in their environment (Figure 10): for all three samples, a KS test is unable to reject the hypothesis that they are drawn from the same parent population.

7. CONCLUSIONS

Jellyfish galaxies are galaxies that exhibit tentacles of material that appear to be stripped from the galaxy and are the most extreme examples of galaxies in the process of being stripped of their gas. We have searched for galaxies whose morphology is suggestive of gas-only removal mechanisms, from extreme jellyfishes to less spectacular examples with evidence of debris tails and morphologies of stripped material or asymmetry suggestive of unilateral external forces. This is the first systematic search for such signatures at low redshift. The purpose of this atlas is to provide a large sample suitable for statistical and follow-up studies that will be able to securely identify the process responsible for the observed morphologies.

This paper presents the largest sample of stripping candidates known to date: 344 galaxies in 71 galaxy clusters of the OMEGAWINGS+WINGS sample, and 75 candidates in groups and lower mass structures in the PM2GC sample, all at $z = 0.04-0.07$. Stripping candidates have been visually selected on the basis of B or V deep images. We present the atlas of single filter and (when available) color-composite images of all candidates, together with catalogs of positions, redshifts, JClass and eventual cluster membership.

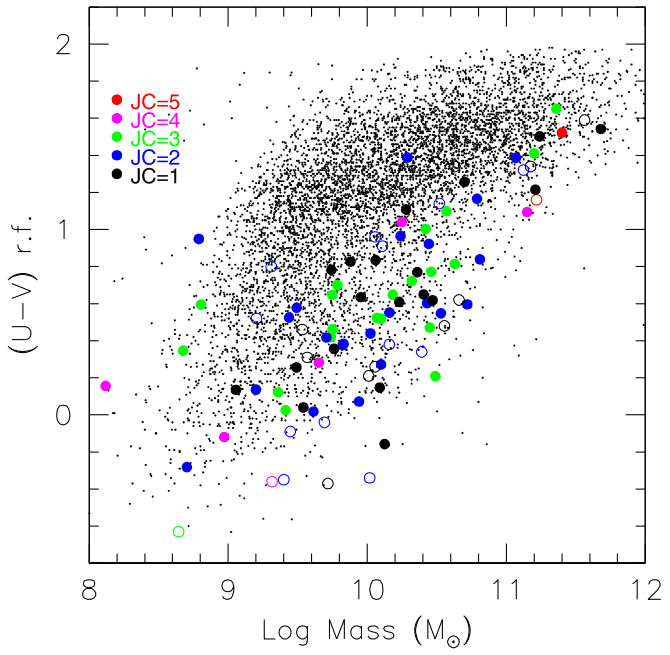

Figure 9. U–V rest frame color–mass diagram for all members of OMEGAWINGS clusters (small black points) and for stripping candidates of different JClasses = 5 red; = 4 magenta; = 3 green; = 2 blue; = 1 black. OMEGAWINGS = filled symbols, WINGS = empty symbols.

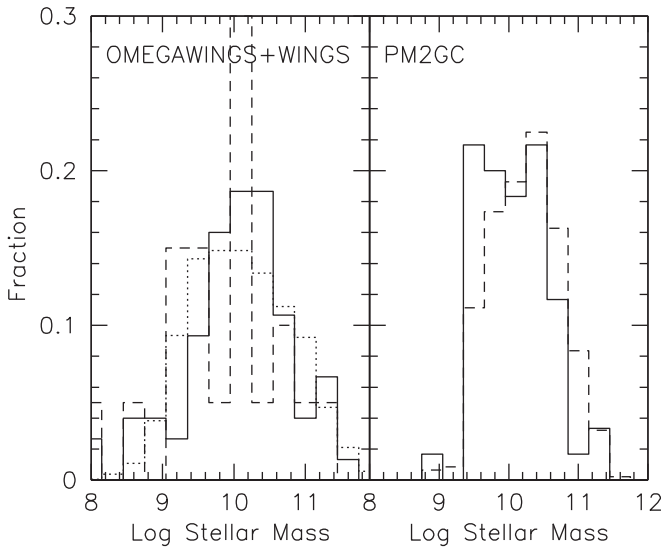

Figure 10. Galaxy stellar mass fractional distribution. (Left) OMEGAWINGS candidates (solid line), WINGS candidates (dashed line) and all cluster members in the OMEGAWINGS+WINGS database (dotted line). (Right) PM2GC candidates (solid line) and all galaxies (dashed line).

Stripping candidates have been found in all clusters inspected, that have σ ranging from ∼500 to ∼1200 km s^{-1}. The number of candidates per cluster does not depend on the cluster σ or L_X, and candidates are found at all clustercentric radii, out to ∼1.5 times the cluster virial radius that is the area covered by our imaging in these clusters. An in-depth analysis of the environments of these galaxies will be presented in a separate paper (Y. Jaffé et al. 2016, in preparation).

While all jellyfishes previously known from the literature are in clusters (but see e.g., Clemens et al. 2000 for a well studied case of ram pressure stripping in a pair), we find striking stripping candidates (highest JClasses) also outside of clusters, in groups and lower mass halos of the PM2GC sample, with masses in the range $10^{11}-10^{14}M_\odot$. However, especially for the lowest JClasses, it is possible that the observed features originate from other mechanisms, such as minor or major mergers and tidal interactions. This result deserves further investigation, to fully understand the role and the cause of gas stripping in groups and its impact on galaxy evolution in general and on the global quenching of SF.

Our preliminary analysis shows that the SFR is enhanced on average by a factor of 2 in stripping candidates compared to non-candidates of the same mass (2.5σ). This suggests that the process responsible for disturbed morphologies consistent with stripping causes a significant increase in the star formation activity. There are a few non-starforming candidates (5%–10%), either in a post-starburst phase or spectroscopically passive, and they display rather weak stripping signatures. Our sample comprises candidates of all masses, from $\log M/M_\odot < 9$ to $>11.5\,M_\odot$, indicating that whatever causes the disturbed morphologies selected in this paper can be effective on galaxies of any mass.

Only Integral Field spectroscopic observations can fully reveal the cause and effects of gas removal in these galaxies, and allow us to measure the stripping timescale, quantify the amount of stars formed in the stripped gas, unanbiguously identify the physical process responsible for the gas outflow and directly study the effects on the evolution of the galaxy. Integral Field Spectroscopy with MUSE/VLT was obtained for two of our OMEGACAM jellyfishes. These data spectacularly reveals the emission lines (Hβ, [O III], N II, Hα and S II) associated with the ionized gas in the trails, out to several tens of kpc from the galaxy. This gas is ionized from the massive stars in the star-formation knots that are visible in the optical images. These results will be presented in a forthcoming paper (Y. Jaffé et al. 2016, in preparation). A larger IFS study on a statistically significant subsample of our candidates is about to start with MUSE (ESO Large Program 196.B-0578) and will unveil the rich physics and implications of the stripping phenomenon in galaxies as a function of galaxy environment and galaxy mass.

We thank the referee, Prof. Harald Ebeling, for his constructive comments and suggestions that helped us improve the clarity and contents of the paper. We thank Joe Liske, Simon Driver and the whole MGC team for making their great data set easily accessible, and Rosa Calvi for all her work on the PM2GC. This work is based on two GTO programs on VST. We thank Massimo Capaccioli, Enrico Cappellaro, Pietro Schipani, Andrea Baruffolo and the whole VST and Omega-CAM teams for making this research possible. This work is based on data obtained with AAOmega on the AAT, and we acknowledge the generous support to the OMEGAWINGS project from the Australian Time Assignment Committee. We acknowledge financial support from a PRIN-INAF 2014 grant. YLJ acknowledges support by FONDECYT grant N. 3130476. BV was supported by the World Premier International Research Center Initiative (WPI), MEXT, Japan and by the Kakenhi Grant-in-Aid for Young Scientists (B)(26870140) from the Japan Society for the Pro- motion of Science (JSPS). This research has made use of the NASA/IPAC Infrared Science Archive and the NASA/IPAC Extragalactic Database (NED), which are operated by the Jet Propulsion Laboratory, California Institute of Technology, under contract with the

National Aeronautics and Space Administration. This publication makes use of data products from the Wide-field Infrared Survey Explorer, which is a joint project of the University of California, Los Angeles, and the Jet Propulsion Laboratory/California Institute of Technology, and NEOWISE, which is a project of the Jet Propulsion Laboratory/California Institute of Technology. WISE and NEOWISE are funded by the National Aeronautics and Space Administration. Funding for SDSS-III has been provided by the Alfred P. Sloan Foundation, the Participating Institutions, the National Science Foundation, and the U.S. Department of Energy Office of Science. The SDSS-III web site is http://www.sdss3.org/. SDSS-III is managed by the Astrophysical Research Consortium for the Participating Institutions of the SDSS-III Collaboration.

REFERENCES

Balogh, M. L., Navarro, J., & Morris, S. 2000, ApJ, 540, 113
Barnes, J. E., & Hernquist, L. 1992, ARA&A, 30, 705
Boselli, A., & Gavazzi, G. 2006, PASP, 118, 517
Bournaud, F., Combes, F., & Jog, C. J. 2004, A&A, 418, L27
Bravo-Alfaro, H., Cayatte, V., van Gorkom, J., & Balkowski, C. 2001, A&A, 379, 347
Byrd, G., & Valtonen, M. 1990, ApJ, 350, 89
Calvi, R., Poggianti, B. M., Fasano, G., & Vulcani, B. 2012, MNRAS, 419, 14
Calvi, R., Poggianti, B. M., & Vulcani, B. 2011, MNRAS, 416, 727
Calvi, R., Poggianti, B. M., Vulcani, B., & Fasano, G. 2013, MNRAS, 432, 3141
Cava, A., Bettoni, D., Poggianti, B. M., et al. 2009, A&A, 495, 707
Cayatte, V., van Gorkom, J., Balkowski, C., & Kotanyi, C. 1990, AJ, 100, 604
Chung, A., van Gorkom, J., Kenney, J. D. P., Crowl, H., & Vollmer, B. 2009, AJ, 138, 1741
Clemens, M. S., Alexander, P., & Green, D. A. 2000, MNRAS, 312, 236
Cortese, L., Marcillac, D., Richard, J., et al. 2007, MNRAS, 376, 157
Cox, T. J., Jonsson, P., Somerville, R. S., Primack, J. R., & Dekel, A. 2008, MNRAS, 384, 386
Cowie, L. L., & Songaila, A. 1977, Natur, 266, 501
Davies, R. D., & Lewis, B. M. 1973, MNRAS, 165, 231
Dekel, A, & Birnboim, Y. 2006, MNRAS, 368, 2
De Lucia, G. 2010, arXiv:1012.3326
Driver, S. P., Liske, J., Cross, N. J. G., De Propris, R., & Allen, P. D. 2005, MNRAS, 360, 81
Ebeling, H., Voges, W., Bohringer, H., et al. 1996, MNRAS, 281, 799
Ebeling, H., Edge, A. C., Bohringer, H., et al. 1998, MNRAS, 301, 881
Ebeling, H., Edge, A. C., Allen, S. W., et al. 2000, MNRAS, 318, 333
Ebeling, H., Stephenson, L. N., & Edge, A. C. 2014, ApJ, 781, 40
Fasano, G., Marmo, C., Varela, J., et al. 2006, A&A, 445, 805
Fasano, G., Vanzella, E., Dressler, A., et al. 2012, MNRAS, 420, 926
Fogarty, L. M. R., Bland-Hawthorn, J., Croom, S. M., et al. 2012, ApJ, 761, 169
Fritz, J., Poggianti, B. M., Bettoni, D., et al. 2007, A&A, 470, 137
Fritz, J., Poggianti, B. M., Cava, A., et al. 2011, A&A, 526, 45
Fritz, J., Poggianti, B. M., Cava, A., et al. 2014, A&A, 566, 32
Fumagalli, M., Fossati, M., Hau, G. K., et al. 2014, MNRAS, 445, 4335
Giovanelli, R., & Haynes, M. P. 1985, ApJ, 292, 404
Gullieuszik, M., Poggianti, B. M., Fasano, G., et al. 2015, A&A, 581, 41
Gunn, J. E., & Gott, J. R. 1972, ApJ, 176, 1
Haynes, M., Giovanelli, R., & Chincarini, G. 1984, ARA&A, 22, 445
Hester, J. A., Seibert, M., Neill, J. D., et al. 2010, ApJL, 716, L14
Ho, I.-T., et al. 2014, MNRAS, 444, 3894
Hopkins, P. F., Cox, T. J., Younger, J. D., & Hernquist, L. 2009, ApJ, 691, 1168
Jaffe, Y., Smith, R., Candlish, G. N., et al. 2015, MNRAS, 448, 1715
Kenney, J. D. P., Abramson, A., & Bravo-Alfaro, H. 2015, AJ, 150, 59
Kenney, J. D. P., & Koopmann, R. A. 1999, AJ, 117, 181
Kenney, J. D. P., van Gorkom, J., & Vollmer, B. 2004, AJ, 127, 3361
Kenney, J. D. P., et al. 2014, ApJ, 780, 119
Kroupa, P. 2001, MNRAS, 322, 231
Larson, R. B., Tinsley, B. M., & Caldwell, C. N. 1980, ApJ, 237, 692
Liske, J., Lemon, D. J., Driver, S. P., Cross, N. J. G., & Couch, W. J. 2003, MNRAS, 344, 307
Lotz, J. M., Jonsson, P., Cox, T. J., & Primack, J. R. 2010a, MNRAS, 404, 575
Lotz, J. M., Jonsson, P., Cox, T. J., & Primack, J. R. 2010b, MNRAS, 404, 590
Machacek, M., Jones, C., Forman, W. R., & Nulsen, P. 2006, ApJ, 644, 155
Mainzer, A., Bauer, J., Grav, T., et al. 2011, ApJ, 731, 53
Merluzzi, P., Busarello, G., Dopita, M. A., et al. 2013, MNRAS, 429, 1747
Mihos, C., & Hernquist, L. 1994, ApJL, 425, L13
Moore, B., Katz, N., Lake, G., Dressler, A., & Oemler, A. 1996, Natur, 376, 613
Moretti, A., Poggianti, B. M., Fasano, G., et al. 2014, A&A, 564, 138
Nulsen, P. E. J. 1982, MNRAS, 198, 1007
Omizzolo, A., Fasano, G., Reverte Paya, D., et al. 2014, A&A, 561, 111
Owers, M., Couch, W. J., Nulsen, P. E. J., & Randall, S. W. 2012, ApJL, 750, L23
Poggianti, B. M., Calvi, R., Bindoni, O., et al. 2013, ApJ, 762, 77
Poggianti, B. M., Smail, I., Dressler, A., et al. 1999, ApJ, 518, 576
Poggianti, B. M., von der Linden, A., De Lucia, G., et al. 2006, ApJ, 642, 188
Rasmussen, J., Ponman, T. J., & Mulchaey, J. S. 2006, MNRAS, 370, 453
Rasmussen, J., Ponman, T. J., Verdes-Montenegro, L., et al. 2008, MNRAS, 388, 1245
Rawle, T. D., Altieri, B., Egami, E., et al. 2014, MNRAS, 442, 196
Rieke, G. H., Alonso-Ferrero, A., Weiner, B. J., et al. 2009, ApJ, 692, 556
Sengupta, C., & Balasubramanyam, R. 2006, MNRAS, 369, 360
Smith, R. J., Lucey, J. R., Hammer, D., et al. 2010, MNRAS, 408, 1417
Sun, M., Vikhlinin, A., Forman, W., Jones, C., & Murray, S. S. 2005, ApJ, 619, 169
Sun, M., Jones, C., Forman, W., et al. 2006, ApJL, 637, L81
Valentinuzzi, T., Woods, D., Fasano, G., et al. 2009, A&A, 501, 851
Varela, J., D'Onofrio, M., Marmo, C., et al. 2009, A&A, 497, 667
Veilleux, S., Cecil, G., & Bland-Hawthorn, J. 2005, ARA&A, 43, 769
Verdes-Montenegro, L., Yun, M. S., Williams, B. A., et al. 2001, A&A, 377, 812
Vijayaraghavan, R., & Ricker, P. M. 2013, MNRAS, 435, 2713
Vollmer, B. 2003, A&A, 398, 525
Vulcani, B., Poggianti, B. M., Aragon-Salamanca, A., et al. 2011, MNRAS, 412, 246
Yagi, M., Yoshida, M., Komiyama, Y., et al. 2010, AJ, 140, 1814
Yoshida, M., Yagi, M., Komiyama, Y., et al. 2008, ApJ, 688, 918
Williams, B. A., & Rood, H. J. 1987, ApJS, 63, 265
Wright, E. L., Eisenhardt, P. R. M., Mainzer, A. K., et al. 2010, AJ, 140, 1868